SULFUR AND PHOSPHORUS DISTRIBUTION BETWEEN LIQUID IRON AND MAGNESIA-SATURATED SLAG IN H_2/H_2O ATMOSPHERE RELEVANT TO A NOVEL GREEN IRONMAKING TECHNOLOGY

by

Mohassab Yousef Mohassab Ahmed

A thesis submitted to the faculty of
The University of Utah
in partial fulfillment of the requirements for the degree of

Master of Science

Department of Metallurgical Engineering

University of Utah

August 2011

UMI Number: 1492327

All rights reserved

INFORMATION TO ALL USERS
The quality of this reproduction is dependent on the quality of the copy submitted.

In the unlikely event that the author did not send a complete manuscript
and there are missing pages, these will be noted. Also, if material had to be removed,
a note will indicate the deletion.

UMI 1492327

Copyright 2011 by ProQuest LLC.

All rights reserved. This edition of the work is protected against
unauthorized copying under Title 17, United States Code.

ProQuest LLC.
789 East Eisenhower Parkway
P.O. Box 1346
Ann Arbor, MI 48106 - 1346

Copyright © Mohassab Yousef Mohassab Ahmed 2011

All Rights Reserved

The University of Utah Graduate School

STATEMENT OF THESIS APPROVAL

The thesis of **Mohassab Yousef Mohassab Ahmed**

has been approved by the following supervisory committee members:

Hong Yong Sohn	, Chair	**05/05/2011** Date Approved
Hang Goo Kim	, Member	**05/05/2011** Date Approved
Michael S. Moats	, Member	**05/05/2011** Date Approved

and by **Jan D. Miller** , Chair of the Department of **Metallurgical Engineering**

and by Charles A. Wight, Dean of The Graduate School.

ABSTRACT

As an integral part of a research project which aimed to develop a novel green ironmaking process, an experimental determination of the sulfur and phosphorus distribution ratios, L_S and L_P, respectively, between molten iron and CaO-$MgO_{(Saturated)}$-SiO_2-Al_2O_3-FeO slag was determined in the temperature range 1550-1650°C. Oxygen partial pressure was controlled by H_2/H_2O equilibrium in the range of 10^{-10}-10^{-8} atm.

For sulfur distribution, it was found that the trend of the distribution is the same as the previous work done under CO/CO_2 atmosphere but L_S in this case is 38-44 times less under similar oxygen partial pressure. This might be attributed to the impact of H_2 on the distribution. Considering the fact that the input sulfur in the proposed process is approximately 34 times less than the blast furnace process, the proposed process would produce hot metal with approximately the same sulfur content to the hot metal produced by the blast furnace.

For phosphorus distribution, L_P was 450-1050 times that of the blast furnace. Also considering the amount of phosphorus input in the two processes, it was found that the expected P content in iron in the new process would be approximately three times less than in the blast furnace hot metal. This means that the proposed process will produce hot metal with much lower phosphorus which will minimize the need for dephosphorization in the steelmaking stage.

TABLE OF CONTENTS

ACKNOWLEDGMENTS

I would like to express my gratitude to my supervisor, Professor H. Y. Sohn, whose expertise, understanding, and patience added considerably to my graduate experience. I appreciate his vast knowledge and skill in many areas and his assistance in writing my first papers in addition to this thesis.

I would like to thank Professor Hang Goo Kim for his expert advice and instructions.

I would like to thank supervisory committee member, Professor Michael S. Moats, for the time and effort to review my work.

I appreciate Professor Mohamed H. Khedr, without whose motivation and encouragement I would not have considered a graduate career.

This research would not have been possible without the financial assistance of American Iron and Steel Institute (AISI) through a Research Service Agreement with the University of Utah under AISI's CO_2 Breakthrough Program.

I am grateful to my parents, parents-in-law, my brother, and my sisters for the support they provided me through my entire life.

Sincere appreciation and thanks go to my beloved wife and best friend, Eman, without whose love, encouragement, and assistance I would not have finished this thesis.

Special thanks go to the light of my life, my daughter. Noor, I am writing this acknowledgment exactly on your first birthday.

I must say thanks to Allah, my God, for uncountable blessings. This thesis is one of them.

I dedicate this work to my grandmother who was my first teacher. Also this thesis is dedicated to the Egyptian people who died on January 25th for the freedom of Egypt.

CHAPTER 1

SULFUR DISTRIBUTION BETWEEN LIQUID IRON AND MAGNESIA-SATURATED SLAG IN H_2/H_2O ATMOSPHERE RELEVANT TO A NOVEL GREEN IRONMAKING TECHNOLOGY

1. 1. Introduction

In recent years, there has been an increased demand for clean steels with low sulfur. It is known that sulfur contributes to drastic decrease of ductility and fracture toughness of steel. There has been much research done to study the distribution of sulfur and the sulfide capacities for various slag compositions, different temperatures and oxygen potential.[1] Most previous work used CO/CO_2 gas mixture to control p_{O_2}.[2-7] Others used only inert atmosphere,[8, 9] although Kor and Richardson[10] used a mixture of CO_2/H_2 to control p_{O_2}. In our group, we are developing a novel green ironmaking process based on the direct gaseous reduction of iron oxide concentrates in a suspension reduction process, with the ultimate goal of significantly reducing CO_2 emission, energy consumption, and environmental pollution in the steel industry[11]. Due to the fact that there is no research done to study sulfur distribution under H_2/H_2O-controlled p_{O_2}, we conducted this research.

Thermodynamics of the desulfurization phenomenon has to be considered on the basis of the partitioning of sulfur between metal and slag phases. Impurities like sulfur or

phosphorus exist in the metallic phase in atomic form while the slags are ionic. Hence, the partition of a species "i" between metal and slag phases will be accompanied by the formation of an ionic species by means of an electrochemical redox reaction, shown by:

$$i\,(\text{metal}) + n\,e^- = i^{n-}\,(\text{slag}) \qquad (1)$$

where n is the valence of the species "i". The above reaction necessitates the participation of electron donors (in other words, cationic species like Ca^{2+} or Mg^{2+}). Thus the concentration of the basic oxides in the slag, or the basicity of the slag, is an important parameter in this reaction. A highly basic slag is expected to provide more electron donors and reaction (1) would be enhanced.

In a simplified way, the sulfur partition reaction can be taken as an exchange reaction between sulfur in the metal and oxygen in the slag:

$$\underline{S}\,(\text{metal}) + O^{2-} = \underline{O}\,(\text{metal}) + S^{2-} \qquad (2)$$

It is noted that the present thermodynamic treatment presupposes that sulfur is present in the slag as sulfide and not as sulfate because of the low oxygen potential prevailing in the system (p_{O_2} is approximately 10^{-10}~10^{-9}).[12]

The equilibrium constant for reaction (2), K_2 is given by the equation:

$$K_2 = \frac{a_{\underline{O}} \cdot a_{S^{2-}}}{a_{\underline{S}} \cdot a_{O^{2-}}} \quad (3)$$

where a is the thermodynamic activity relative to appropriate standard states. The activities of sulfur in the two phases can be expressed in terms of the concentrations, viz.

$$a_S = (wt\%\underline{S}\ in\ metal).f_{\underline{S}} \quad (4)$$

and

$$a_{S^{2-}} = (X_S\ in\ slag).\gamma_{S^{2-}} \quad (5)$$

where $f_{\underline{S}}$ and $\gamma_{S^{2-}}$ represent the activity coefficients of sulfur in the metal and the sulfide ion in the slag, respectively, and X_S represents sulfur mole fraction in the slag. The sulfur partition ratio L_S is then given by the relationship:

$$L_S = \frac{(wt\%S)_{slag}}{[wt\%\underline{S}]_{in\ metal}} = K_2 . \frac{a_{O^{2-}}}{a_O} . \frac{f_S}{\gamma_{S^{2-}}} \quad (6)$$

To evaluate L_S, it is necessary to know the activities and activity coefficients in Eq. (6) as well as the equilibrium constant K_2. As it is not realistic to attempt to measure these parameters, the problem is approached by considering the equilibrium between the slag and a gas phase where the chemical potentials of relevant species are known and fixed. This has resulted in the development of the concept of slag capacity.

The ability of a slag to absorb a given species is normally expressed as "Slag – Capacity." In the case of sulfur transfer, this would be referred to as the sulfide capacity. The concept of sulfide capacity, since its inception by Fincham and Richardson,[12] has been widely used by steelmakers in connection with the desulfurization of steel. According to these authors, the sulfide capacity of slag is expressed as:

$$C_S = \exp(\frac{-\Delta G^\circ}{RT})(\frac{a_{O^{2-}}}{f_{S^{2-}}}) \quad (7)$$

where $a_{O^{2-}}$ is the activity of oxygen ion in the slag, $f_{S^{2-}}$ is the activity coefficient of sulfide ions in the slag, R is the gas constant, T is the temperature in K, and ΔG° is the standard Gibbs free energy change for the following reaction:

$$\frac{1}{2}S_2(g) + O^{2-}(slag) = S^{2-}(slag) + \frac{1}{2}O_2(g) \quad (8)$$

where

$$\Delta G^\circ = 118535 - 58.8157 \times T \ (J/mol) \quad (9)$$

In terms of measurable quantities, the sulfide capacity can be expressed as:

$$C_S = (wt\%S_{slag})(\frac{p_{O_2}}{p_{S_2}})^{1/2} \quad (10)$$

While the exponential factor on the right side of Eq. (7) is system independent, the ratio $a_{O^{2-}} / f_{S^{2-}}$ is characterized by the specific system. Fincham and Richardson[12] assumed the constancy of the above ratio for a given slag. While Richardson's justification of $a_{O^{2-}}$ being constant due to polymerization/depolymerization reactions in silicate melts is acceptable, the term $f_{S^{2-}}$ need not be constant. Any modeling of the sulfide capacities for complex slags must take into account this variation and thus the sulfide capacities are difficult to predict purely on the basis of the thermodynamics of the silicate melts alone, unless the activity coefficient of the sulfide ion is indirectly taken into consideration.

The concept of sulfide capacity is valid for $p_{O_2} < 10^{-6}$ atm at 1500°C when the sulfur is stabilized in the slag as sulfide. At higher partial pressures, sulfate would be more stable and the corresponding slag metal reaction would be:

$$\frac{1}{2}S_2(g) + \frac{3}{2}O^{2-}(slag) = SO_4^{2-}(slag) \qquad (11)$$

At this higher oxygen potential, an expression for the sulfate capacity can be written in a corresponding manner:

$$C_{SO_4^{2-}} = \frac{(Wt\%S)}{(p_{O_2})^{3/2}(p_{S_2})^{1/2}} \qquad (12)$$

In the case of iron- and steelmaking processes, it is the sulfide capacity value of the slag that is of great relevance. The C_S values of a number of synthetic slags have been experimentally measured from the 1950s. These have been periodically reviewed.[13-15] In general, as seen from Eq. (7), the sulfide capacity of slag is a function of the activity of the oxygen in the slag, which in turn, is dependent on the slag basicity. The expression:

$$B = \frac{(wt\%\, CaO)}{(wt\%\, SiO_2)} \tag{13}$$

is used in this study.

As mentioned earlier, the concept of sulfide capacity is based on gas/slag equilibration. In order to develop a relation between C_S and L_S, Eqs. (7) and (8) are to be combined suitably. This is enabled by a consideration of the solubility of sulfur and oxygen in the hot metal according to:

$$\frac{1}{2} S_2(g) = \underline{S}(metal) \tag{14}$$

$$\frac{1}{2} O_2(g) = \underline{O}(metal) \tag{15}$$

The equilibrium constants for the above equations can be represented as:

$$K_{14} = \frac{a_{\underline{S}(metal)}}{p_{S_2}^{0.5}} \quad (16)$$

$$K_{15} = \frac{a_{\underline{O}(metal)}}{p_{O_2}^{0.5}} \quad (17)$$

These equilibrium constants can be combined with the expression for sulfide capacity to obtain a relationship for the sulfur partition ratio between the hot metal and the slag:

$$\frac{wt\%S\,(in\,slag)}{a_S\,(in\,metal)} = \frac{C_S}{a_O\,(in\,metal)} \cdot \frac{K_{15}}{K_{14}} \quad (18)$$

By substituting Eqs. (16) and (17) for the equilibrium constants, the following expression for the partition ratio, L_S, is obtained:

$$L_S = \frac{(wt\%S)_{slag}}{[wt\%\underline{S}]_{in\,metal}} = \frac{C_S \cdot f_S \cdot K_{15}}{a_O \cdot K_{14}} \quad (19)$$

1. 2. Experimental Details

1. 2. 1. Materials

Table 1-1 shows the chemicals used in the study. CaO was calcined in platinum crucibles at 1200°C for 12 hours to decompose any hydroxide and carbonate present. It was then stored in a desiccator with dry powders of SiO_2, Al_2O_3, MgO, FeO,

Table 1-1. Materials used in the present study.

Material	Purity	Supplier
Aluminum Oxide, (Al_2O_3)	99.99%	Acros Organics (Morris Plains,NJ)
Calcium Oxide, (CaO)	99.95%	Alfa Aesar (Ward Hill, MA)
Silicon(IV) Oxide, (SiO_2)	99.995%	Alfa Aesar (Ward Hill, MA)
Magnesium Oxide, (MgO)	99.99%	Acros Organics (Morris Plains,NJ)
Iron(II) Oxide, (FeO)	99.95%	Sigma-Aldrich (St Louis, MO)
Calcium Pyrophosphate, ($Ca_2P_2O_7$)	≥99.9%	Sigma-Aldrich (St Louis, MO)
Iron(II) Sulfide, (Fees)	99.98	Alfa Aesar (Ward Hill, MA)
Water, H_2O	99.9997	Sigma-Aldrich (St Louis, MO)
Hydrogen, H_2	99.999%	Airgas (Denver, CO)
Sulfur Dioxide, SO_2	99.95	Alexander Chemical Co. (Downers Grove, IL)
Nitrogen, N_2	99.999%	Airgas (Denver, CO)

$Ca_2P_2O_7$,FeS, and Fe. The pure water was used to prevent any scale forming and as a result the potential blocking of the system.

1. 2. 2. Slag Preparation

Required amounts of CaO, SiO_2, Al_2O_3, and MgO were uniformly mixed in an alumina agate mortar to obtain the desired compositions and transferred to graphite crucibles[16] to be premelted at 1600°C for 1 hour under a N_2 flow. The premelted slag was crushed into fine powder using the alumina agate mortar. Premelting has been confirmed by light polarizing microscope and XRD, shown in Figure 1-1, where we should have gehlenite and akermanite phases according to the phase diagram.[17]

Then, the slag powder was transferred into an 99.8% alumina boat to be decarburized[18] at 1200°C for 24 hours under an air flow. Dry FeO, $Ca_2P_2O_7$, and FeS were added and mixed well, and the synthetic slag was stored in a desiccator to be used in the experiments.

1. 2. 3. Experimental Apparatus

The system was composed of two horizontal furnaces connected in series. The first furnace was used as part of a steam generator shown in Figure 1-2. The second furnace was the main reactor shown in Figure 1-3.

1. 2. 4. Steam Generator

Hydrogen and sulfur dioxide gases and liquid water were mixed via a cross connection to go through a 1/8’ ID tube to be introduced to a small furnace kept at 400°C. This

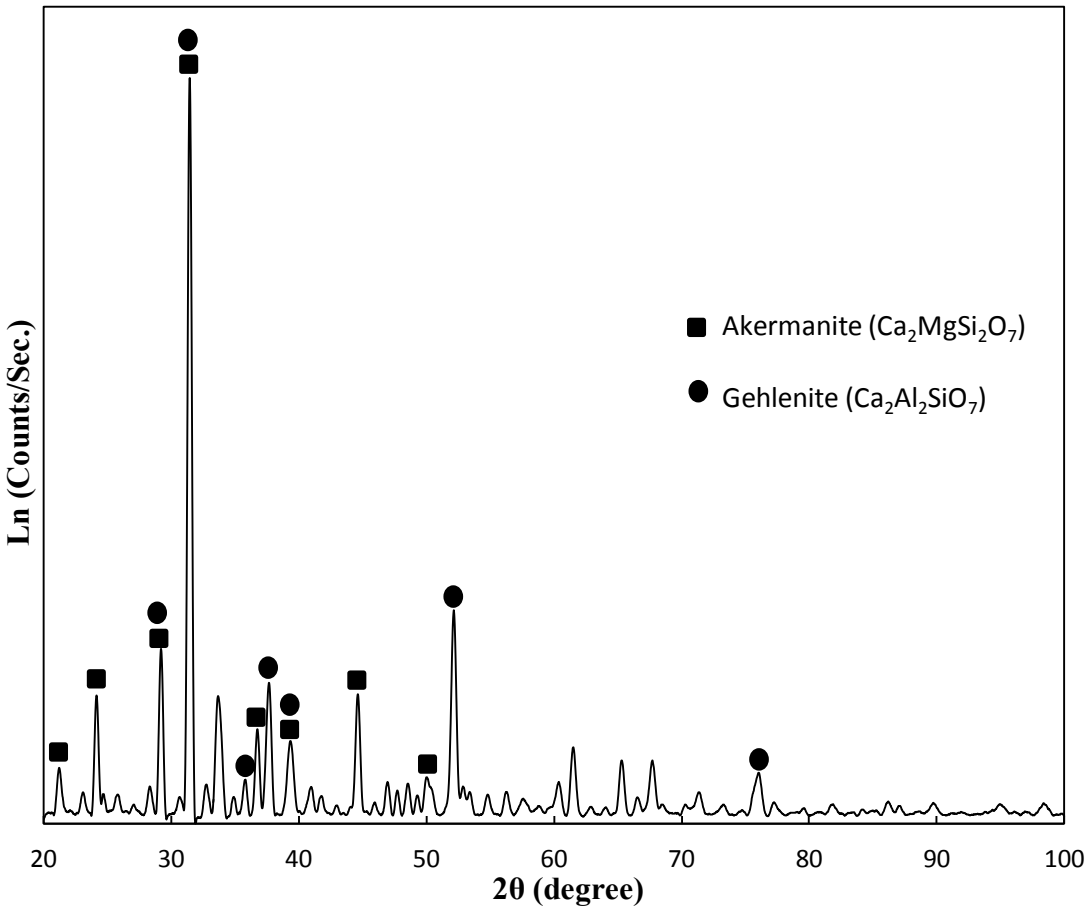

Figure 1-1. XRD pattern shows the peaks for gehlenite and akermanite which ensures the slag premelting according to the phase diagram.[17]

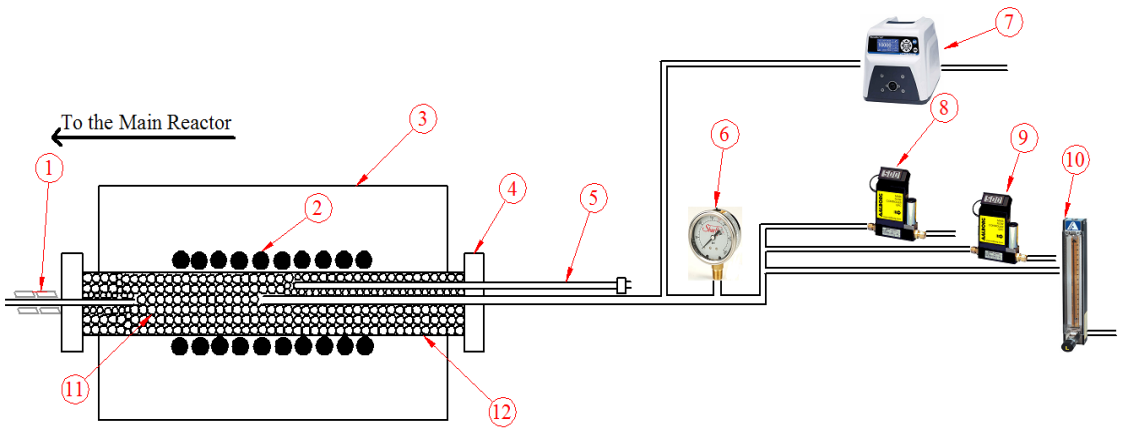

Figure 1-2. The steam generator unit: (1) Heating Tape (2) Heating elements, (3) Furnace body, (4) Stainless steel flange, (5) K-type thermocouple, (6) Pressure guage, (7) Digital water pump, (8) SO_2 mass flow controller (MFC), (9) H_2 MFC, (10) N_2 flow meter, (11) Ceramic rings, (12) Stainless steel tube.

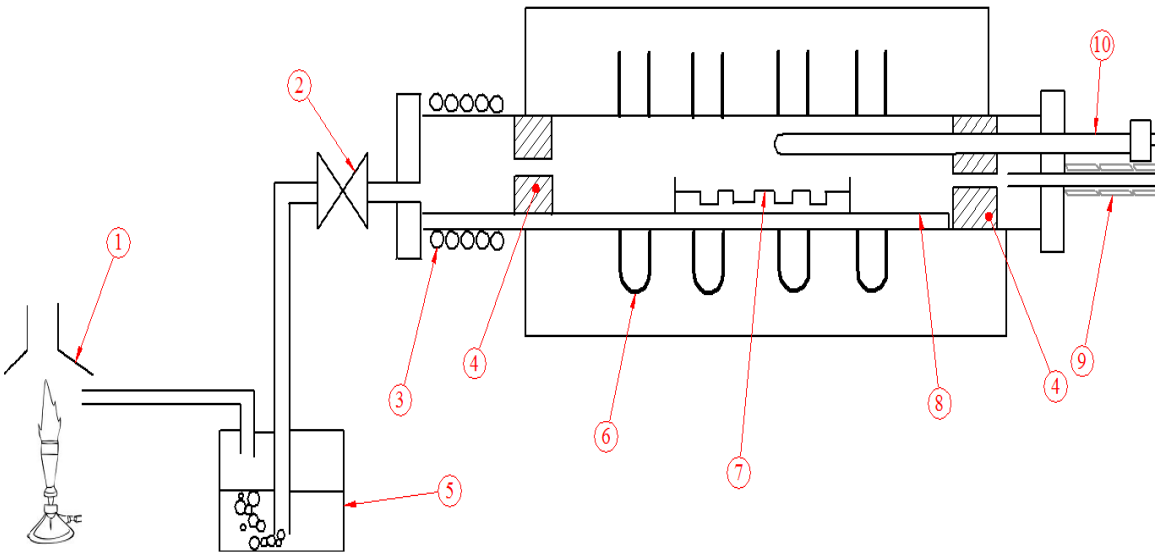

Figure 1-3. Main reactor: (1) Fume hood, (2) Valve, (3) Water cooling jacket, (4) Alumina shield, (5) NaOH scrubber, (6) $MoSi_2$ heating elements, (7) Alumina sample holder, (8) Alumina gutter, (9) Heating tape, (10) B-type thermocouple.

furnace has a 304 stainless steel tube (42 cm/length and 3 cm/ID) full of raschig rings to enhance gases mixing and heat transfer. Then the gas mixture was delivered to the main reactor. The temperature was controlled using a K-type thermocouple and digital temperature controller with PID adjustment and an accuracy of ±2°C.

Water was injected as liquid using a MASTERFLEX digital peristaltic pump drive which provides flow rates from 0.001 mL/min to 3400 mL/min using the same brand pump head with an accuracy of ± 0.01 rpm.

1. 2. 5. Main Reactor

A horizontal electric resistant furnace heated by $MoSi_2$ heating elements with an alumina reaction tube (8 cm/OD, 7cm/ID, 120 cm/length) was employed. Temperature was controlled and monitored inside the tube by two B-type thermocouples (Pt6%Rh/Pt30%Rh). One connected to a 708P temperature controller with an advanced PID adjustment to control the supplied power with an accuracy of ±1°C. The other thermocouple monitored the experimental temperature in the vicinity of the samples with a temperature deviation of 0.2 - 0.5°C. The samples holder was placed in the even temperature zone of the furnace, which was about 15 cm at the center of the reaction tube.

With the help of Aalborg MFC, the flow rates of the SO_2 and H_2 gases were controlled with an accuracy of ±0.1 and ±2 mL/min, respectively.

1. 2. 6. Experimental Procedure

The initial slag composition other than FeO was chosen to be close to that of the blast furnace, which would be used in the new process under development. The temperature range was chosen to be 1550-1650°C which was wide enough to encompass the expected operating temperature. The ratio of H_2 /H_2O was chosen in the range of 1.7-10 to include the expected operating condition and clarify its effect over a much wider range.

The samples were prepared as 2.5 g of slag mixed well with 2.5 g of iron powder. They were mixed well to reduce the time to reach equilibrium in magnesia crucibles (1.8 cm/OD, 4 cm/height, 0.25 cm/wall thickness) supplied by Ozark Technical Ceramics, Inc. (Webb City, MO). The furnace was heated to the target temperature under a flow of N_2. At the target temperature, the furnace was opened to introduce the four-sample alumina holder to the even temperature zone within less than 5 minutes. Then, N_2 was switched to the experimental gases starting with H_2, followed by SO_2 and H_2O. After 10 hours, the experimental gases were switched back to N_2 by stopping the water pump and gradually decreasing the H_2 and SO_2 while increasing the N_2. After 5 minutes of purging, the furnace was opened, the holder was pulled out within 5 minutes, and the samples were quenched in water. Each crucible was carefully crushed and metallic iron was separated from slag. Then the metallic iron was sent for analysis while the slag was finely ground and properly stored for analysis.

Metallic iron was analyzed for sulfur by ICP-OES as well as the entire slag composition. Prior to analysis, the samples were digested in closed Savillex® microwavable vessels. Twelve iron and slag samples were analyzed for sulfur by LECO

C/S analyzer and the results were in good agreement with the ICP results. The chemical analysis results are listed in Table 1-2. In previous research, 6[19] and 8[20] hours were found to be sufficient for similar sample size. To assure 3-phase (gas-slag-metal) equilibrium, 10 hours was chosen in this work.

Table 1-3 lists the oxygen and sulfur partial pressures for the H_2-H_2O-SO_2 gas mixture at the experimental temperatures calculated by HSC 5.11 (Outokumpu Oyj, Riihitontuntie 7, Finland), where 15 corresponding gaseous species were taken into consideration.

Comparing our gas rate/ reactor volume to the previous work,[2-7, 12] it was found that this ratio in our system is smaller. Thus, we could also assume that gases are in equilibrium with each other as well as with the condensed phases.

Reproducibility of the experiments was confirmed by the consistency of the results of repeated experiments under the same conditions, as shown in Figure 1-4.

1. 3. Results and Discussion

The effect of basicity, oxygen potential, and temperature on sulfur distribution ratio will be discussed. Also, the blast furnace will be compared to the proposed process for L_S. From previous research,[21] water has a significant solubility in slag, indicating that it could affect the L_S. This made it difficult to obtain predictions using any of the available models since none of them included the effect of water solubility in slag.

Table 1-2. The chemical analysis of the samples.

Sample	(S)%	FeO%	MgO%	CaO%	Al_2O_3%	SiO_2%	[S]%	T^0C	Log(Ls)
S1	1.55	25.3	17.3	20.7	6.26	29.8	11.9	1550	-0.89
S2	2.72	35.4	12.9	20.6	6.72	24.6	6.11	1550	-0.35
S3	2.88	33.1	11.7	26.3	7.81	28.5	7.16	1550	-0.40
S4	4.77	41.3	10.8	21.5	6.20	21.0	6.03	1550	-0.10
S5	0.93	21.6	19.2	20.9	8.74	28.3	7.15	1550	-0.89
S6	1.01	19.9	20.2	23.0	7.99	33.0	6.96	1550	-0.84
S7	1.85	22.3	15.2	29.8	9.48	26.4	7.79	1550	-0.62
S8	2.03	20.7	10.6	32.1	9.35	23.7	6.21	1550	-0.10
S9	1.08	11.5	22.4	24.9	8.18	32.3	11.2	1550	-1.02
S10	1.34	12.0	18.7	29.0	9.71	29.9	9.67	1550	-0.86
S11	1.56	12.4	17.0	30.9	10.7	29.0	9.32	1550	-0.78
S12	2.16	14.2	14.5	34.7	9.82	31.0	9.38	1550	-0.64
S13	0.81	12.2	22.5	25.1	9.41	32.6	8.43	1550	-1.02
S14	1.20	12.6	16.9	27.4	8.77	39.7	8.28	1550	-0.84
S15	2.27	18.7	15.4	34.7	10.2	16.4	8.42	1550	-0.57
S16	1.72	15.3	16.3	32.4	10.4	28.4	9.49	1550	-0.74
S17	4.17	41.1	15.1	15.8	6.15	19.5	6.85	1600	-0.22
S18	3.44	34.6	13.6	20.4	7.37	24.4	6.69	1600	-0.29
S19	4.81	42.8	11.3	18.1	6.25	17.0	5.59	1600	-0.06

Table 1-2. Continued.

Sample	(S)%	FeO%	MgO%	CaO%	Al_2O_3%	SiO_2%	[S]%	T^0C	Log(Ls)
S20	5.26	52.8	12.4	14.9	4.90	12.2	4.99	1600	0.02
S21	1.31	20.4	22.6	20.7	7.55	27.7	10.2	1600	-0.89
S21	2.12	20.3	22.6	20.7	8.63	27.6	6.08	1600	-0.46
S22	2.52	27.1	15.7	22.7	8.24	23.5	9.42	1600	-0.57
S22	1.66	27.0	17.6	22.6	8.23	23.2	8.24	1600	-0.69
S23	3.55	29.7	14.2	26.2	8.77	22.0	9.20	1600	-0.41
S23	2.37	29.7	14.2	23.7	8.34	22.0	8.83	1600	-0.57
S24	4.46	31.1	14.7	24.9	7.93	21.7	10.1	1600	-0.35
S25	0.78	8.7	25.5	24.3	9.71	36.0	5.60	1600	-0.85
S26	1.17	9.3	21.2	27.1	9.83	31.5	5.30	1600	-0.66
S27	1.80	11.8	18.7	29.1	10.1	28.2	7.45	1600	-0.62
S28	2.48	13.2	19.4	31.0	9.89	23.9	6.26	1600	-0.40
S29	1.02	7.1	23.9	23.9	9.62	31.5	8.56	1600	-0.92
S30	1.77	14.7	20.9	25.5	9.55	28.9	9.71	1600	-0.74
S31	1.97	14.9	25.3	25.2	8.90	23.6	9.37	1600	-0.68
S37	1.34	32.6	20.5	17.8	7.62	23.5	4.85	1650	-0.56
S38	4.15	47.5	14.2	13.5	5.52	16.3	4.71	1650	-0.06

Table 1-3. Oxygen and sulfur partial pressures calculated at the experimental temperatures.
(1 atm = 101.325 kPa)

H_2/ H_2O (molar ratio)	p_{O_2} (atm)			p_{S_2} (atm)			Flow Rates (mL/min)		
	1550ºC	1600ºC	1650ºC	1550ºC	1600ºC	1650ºC	H_2	H_2O	SO_2
1.7	2.2×10^{-09}	4.8×10^{-09}	-	1.4×10^{-03}	1.7×10^{-03}	-	125	0.047	5.7
3.0	7.0×10^{-10}	1.8×10^{-09}	4.2×10^{-09}	1.0×10^{-03}	1.3×10^{-03}	1.6×10^{-03}	149	0.032	5.7
6.0	2.4×10^{-10}	5.3×10^{-10}	-	8.3×10^{-04}	1.0×10^{-03}	-	170	0.018	5.7
10.0	1.1×10^{-10}	2.7×10^{-10}	-	7.3×10^{-04}	9.5×10^{-04}	-	181	0.011	5.7

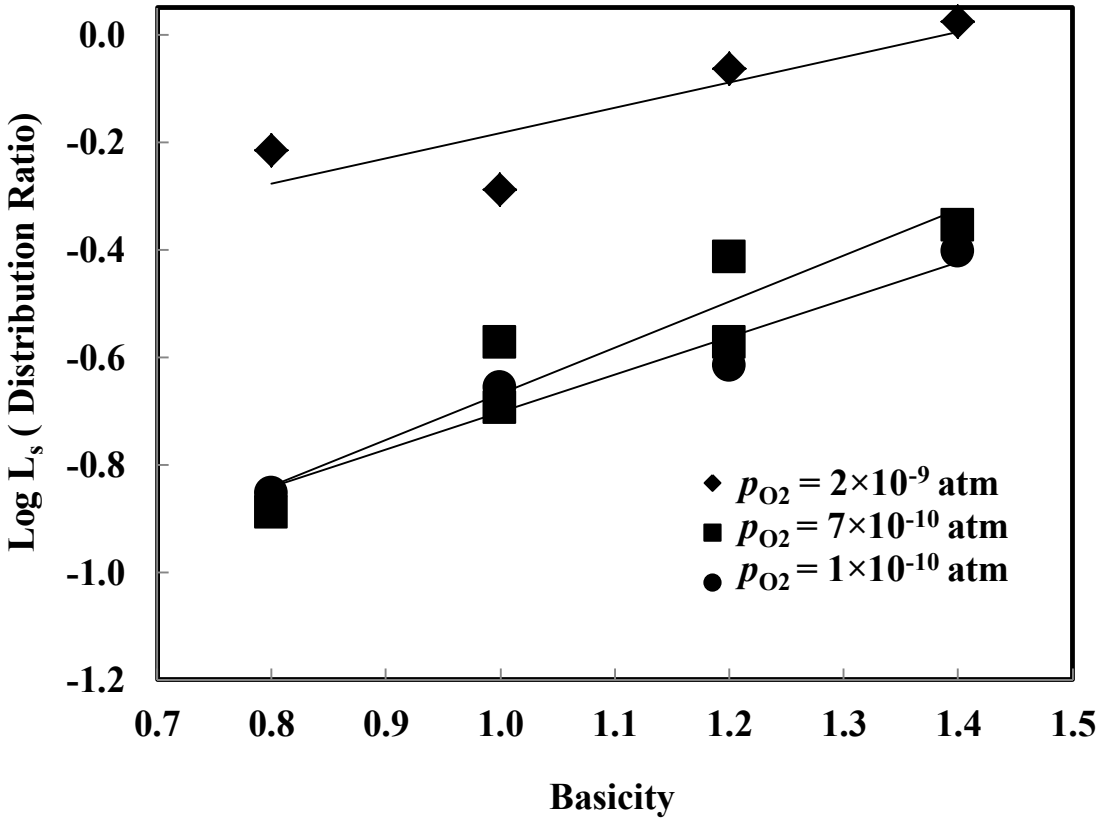

Figure 1-4. The effect of basicity on L_S at 1550^0C and different gas compositions.

1. 3. 1. Effect of Basicity

The effect of basicity on the sulfur partition is shown in Figures 1-4 – 1-6 which indicate that the higher the basicity, the higher the L_S. This is the same trend as for other systems that used CO_2/CO equilibrium.[2-7] That is because a larger amount of CaO leads to higher O^{2-} which captures sulfur dissolved in the metal, as shown in reaction (2). Since both slag composition and p_{O_2} were different from the present conditions, it was difficult to directly compare the results to the previous work.

1. 3. 2. Effect of Oxygen Potential

Figures 1-7 – 1-10 show the effect of oxygen potential on L_S. The trend was similar to thermodynamics expectation according to reaction (2), which indicates that L_S increases with oxygen activity. Considering the difficulty of the direct comparison of our results to the previous results, in addition to the fact that the available theoretical models either use adjustable model parameters as the KTH model[7, 16, 22, 23] or are limited to certain range of compositions or even different slag components,[2, 15, 24, 25] it was found that further theoretical study is needed to develop a model to predict the L_S under H_2/H_2O atmosphere.

1. 3. 3. Effect of Temperature

It is shown in Figure 1-11 that L_S increased with temperature increase at constant input gas composition and basicity which is consistent with the previously reported results.[2-7] This relationship was expected from Eqs. (7) and (19).

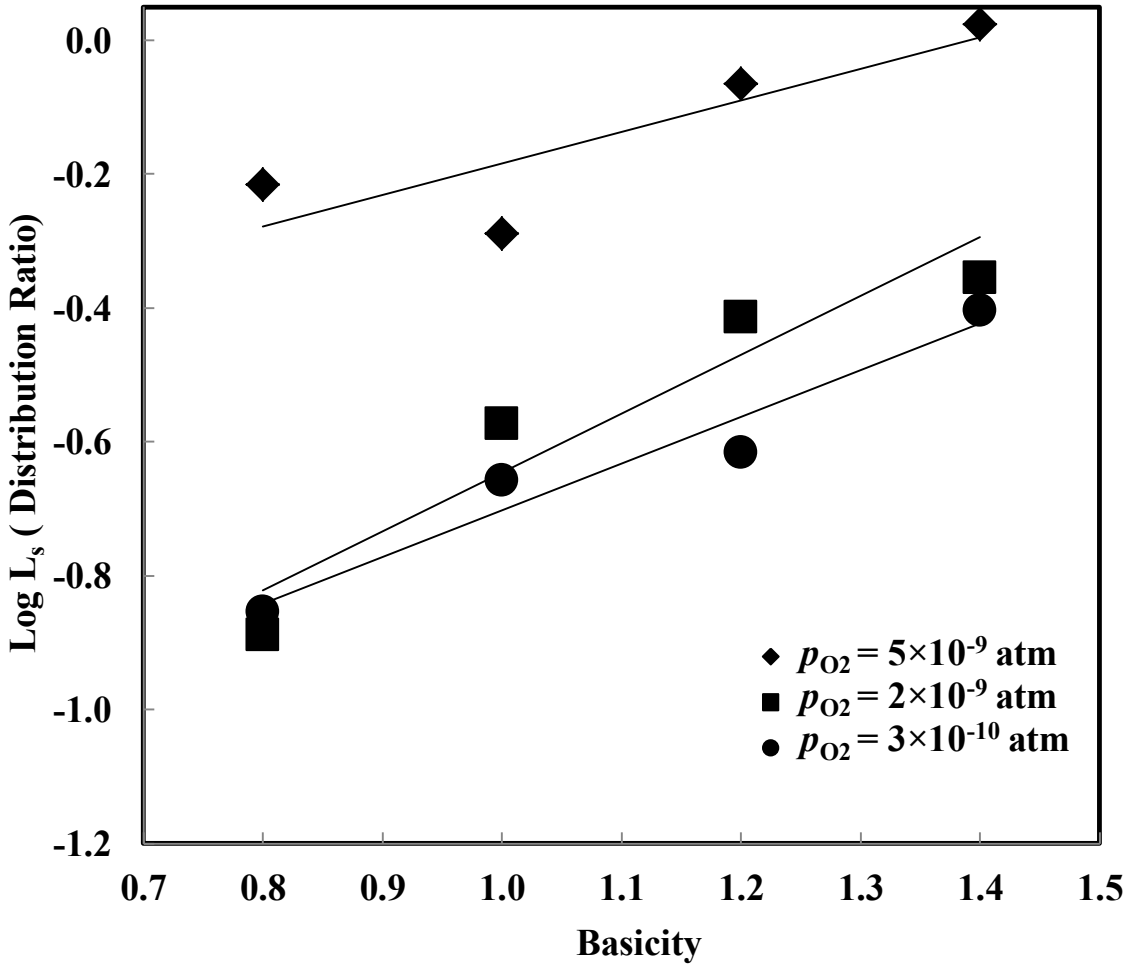

Figure 1-5. The effect of basicity on L_S at 1600°C and different gas compositions.

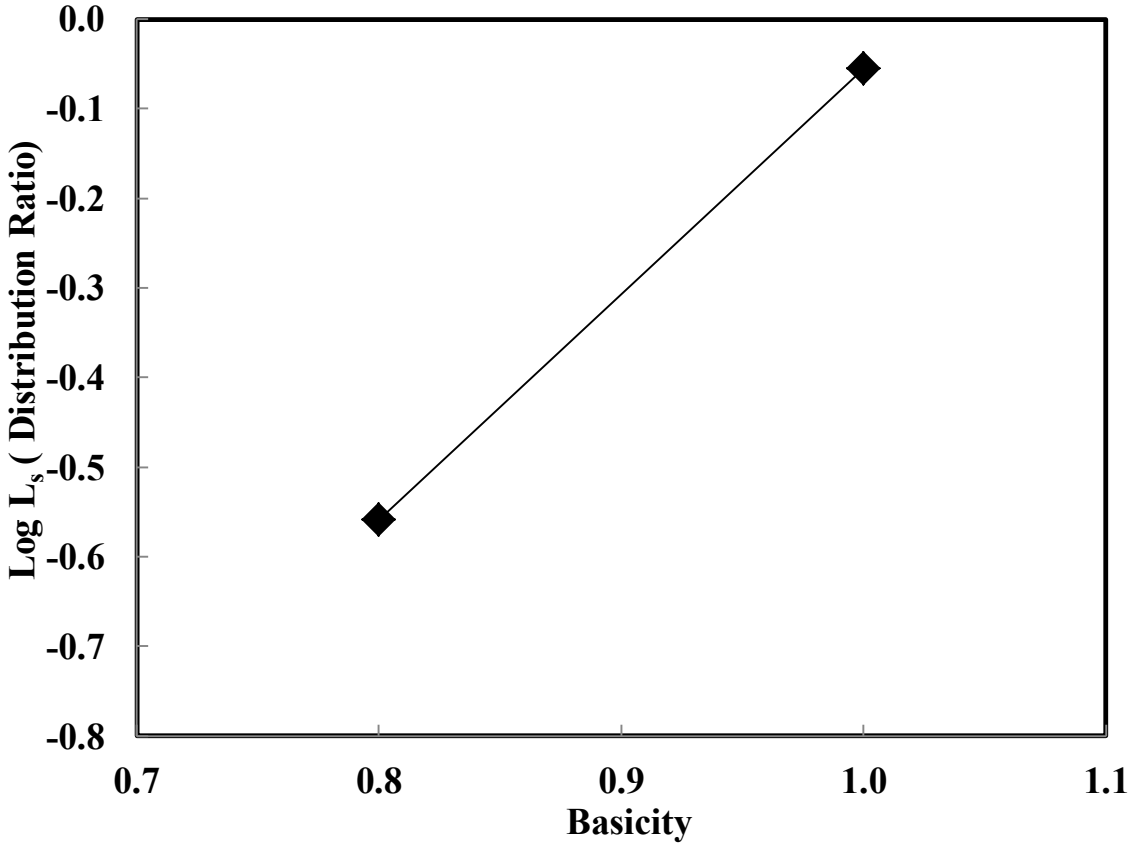

Figure 1-6. The effect of basicity on L_S at 1650°C and $p_{O_2} = 4\times10^{-9}$ atm.

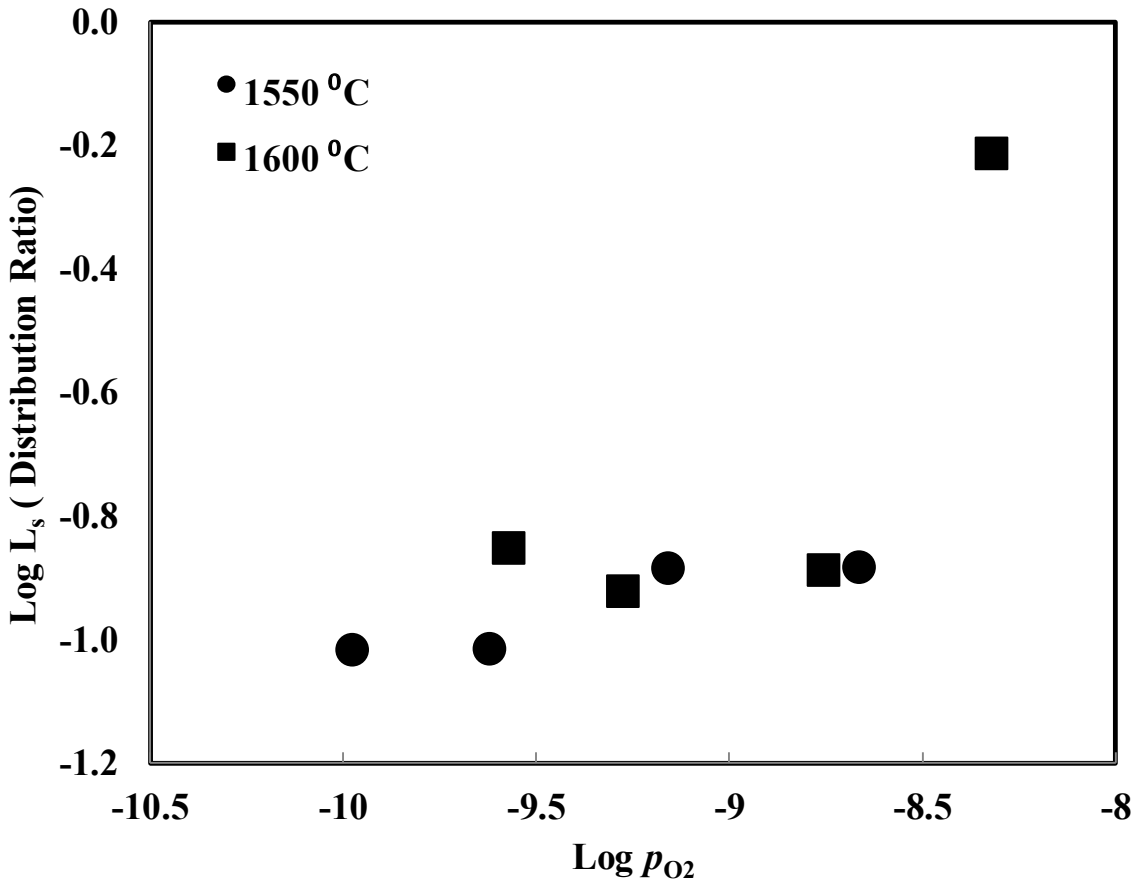

Figure 1-7. The effect of oxygen potential on sulfur distribution factor at basicity of 0.8 at 1550°C and 1600°C.

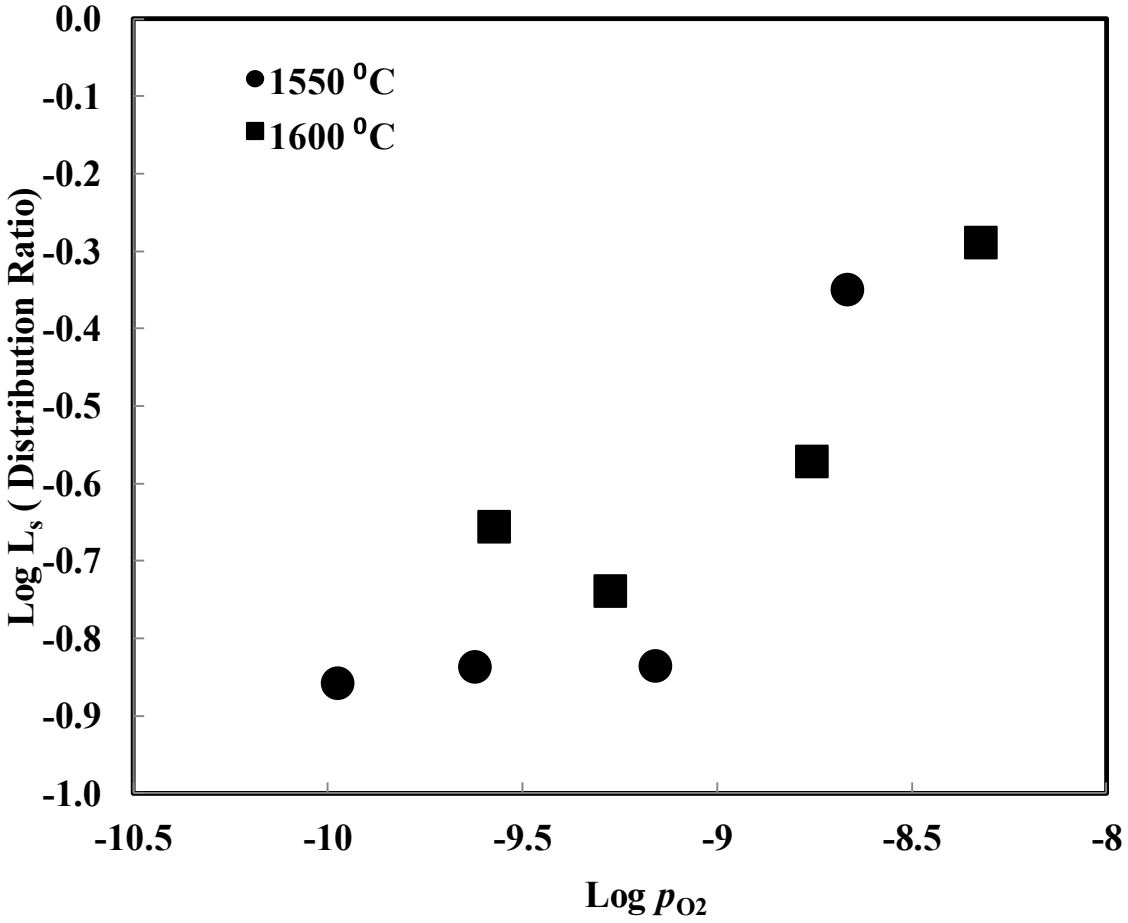

Figure 1-8. The effect of oxygen potential on sulfur distribution factor at basicity of 1 at 1550°C and 1600°C.

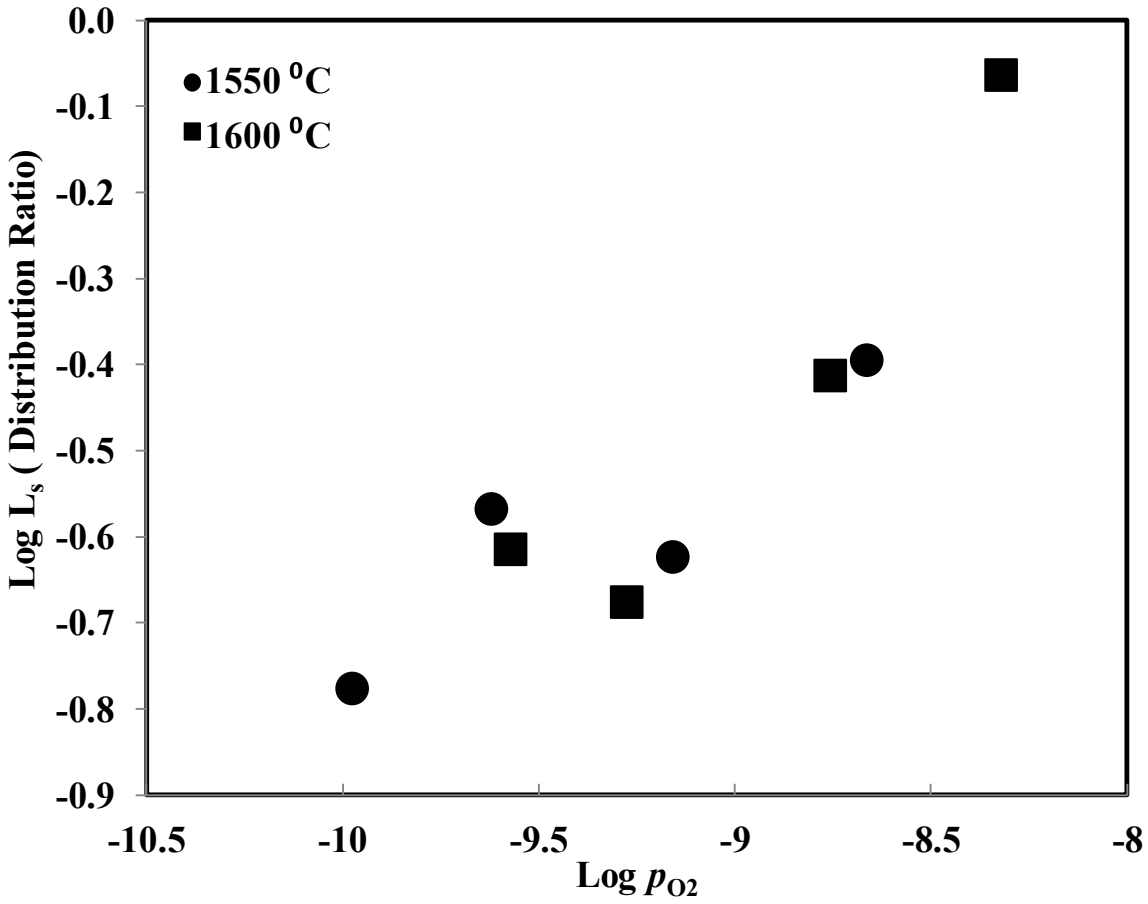

Figure 1-9. The effect of oxygen potential on sulfur distribution factor at basicity of 1.2 at 1550^0C and 1600^0C.

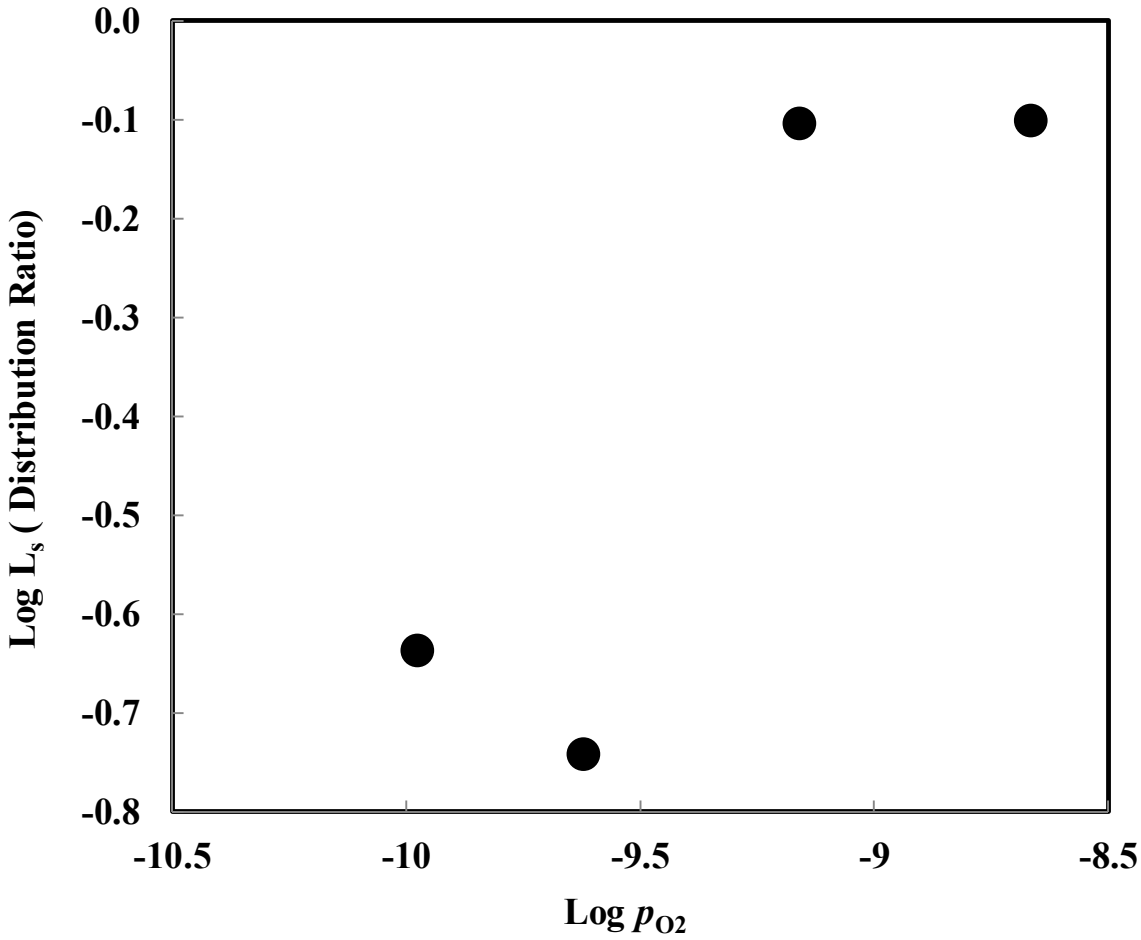

Figure 1-10. The effect of oxygen potential on sulfur distribution factor at basicity of 1.4 at 1550 °C.

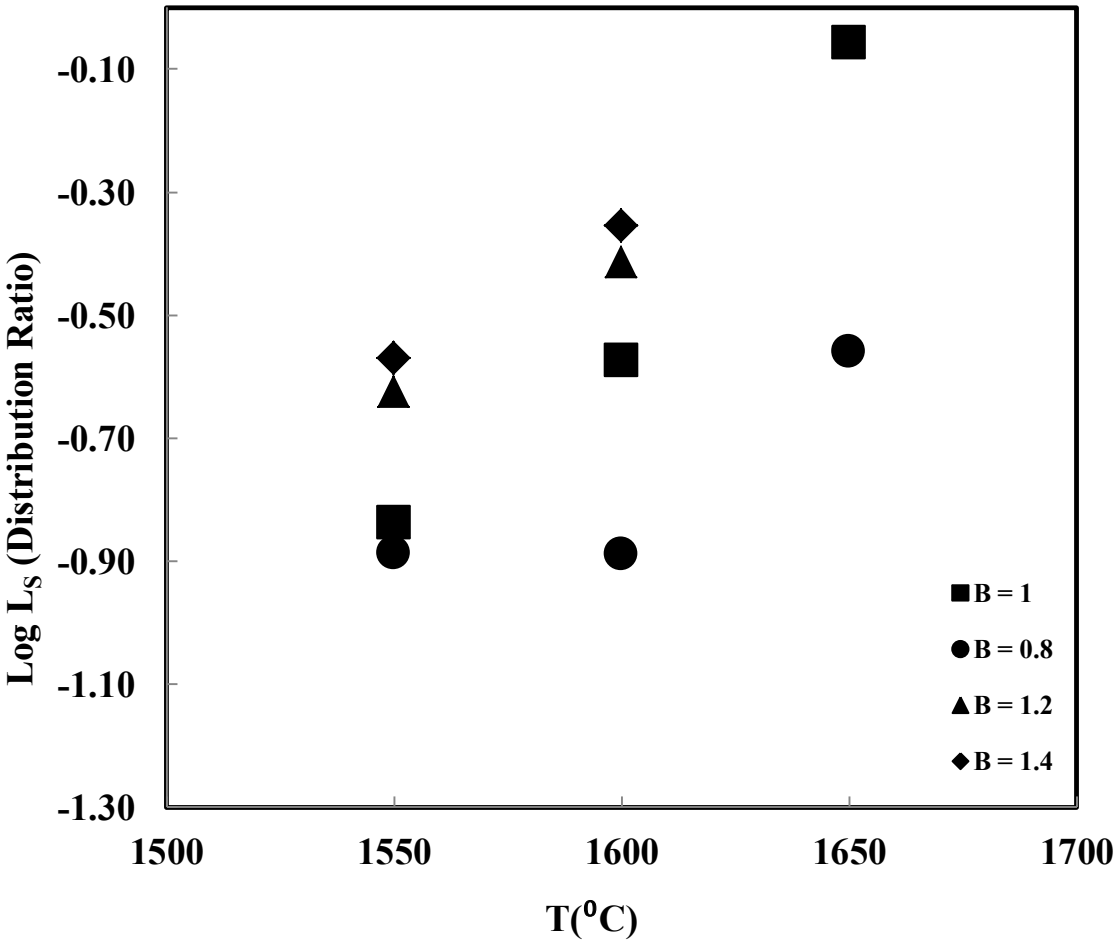

Figure 1-11. The effect of temperature on L_S at $H_2/H_2O = 3$ and differnet basicities.

1. 3. 4. Blast Furnace Versus the Proposed Green Ironmaking Technology

Shankar[25] collected blast furnace data from the G furnace of Tata Steel and found that the LS was in the range of 15-35. In this study, L_S in the range of 0.4-0.8 at and are 2.2×10-09 and 1.4×10-03, respectively, and the temperature was 1550^{0}C (samples 1-4 in Table 1-3). These conditions are the closest to the proposed conditions of the green ironmaking process. Also, one major difference between the blast furnace slag and the proposed process slag is the total iron which is < 4 wt% in the blast furnace slag and 26-43 wt% in samples 1-4. This means in the proposed process, the LS is 38-44 times less than the blast furnace. Considering the amount of sulfur input in the two processes where the proposed process has sulfur of approximately 0.02 wt% in ore,[26] while the main sources of sulfur in the blast furnace are the coke in addition to the ore. Coke contains an average of 0.65 wt% sulfur.[27] This means that the input sulfur in the proposed process is approximately 34 times less than the blast furnace, indicating that the proposed process would produce hot metal with sulfur content close to the hot metal produced by the blast furnace. For this reason, further research will be carried out to develop the optimum conditions to minimize sulfur in hot metal under H_2/H_2O atmosphere.

1. 4. Conclusions

In the present work, the sulfur distribution factor (L_S) between molten iron and CaO-$MgO_{(Saturated)}$-SiO_2-Al_2O_3-FeO slag was determined in the temperature range 1550-1650°C. Oxygen partial pressure was controlled by H_2/H_2O equilibrium in the range of 10^{-8}-10^{-10} atm. It was found that the trend of the distribution was similar to the previous work and L_S was 38-44 times less than in the blast furnace. From previous research,[21]

water has a significant solubility in slag, indicating that it should affect the L_S. Due to the fact that the input sulfur in the proposed process is approximately 34 times less than the blast furnace process, the proposed process would produce hot metal with approximately the same sulfur content to the hot metal produced by the blast furnace. Further study should be carried to study the impact of H_2 and H_2O on L_S.

1. 5. References

1. Y. Kang and A. Pelton: Thermodynamic model and database for sulfides dissolved in Molten Oxide Slags, *Metall. Mater. Trans*. B, 2009, vol. 40 (6), pp. 979-94.

2. Y. Taniguchi: Sulphide capacities of CaO-Al_2O_3-SiO_2-MgO-MnO slags in the temperature range 1 673 - 1 773K, *ISIJ Int.*, 2009, vol. 49 (2), pp. 156-63.

3. A. Shankar, M. Görnerup, S. Seetharaman and A. Lahiri: Sulfide capacity of high alumina blast furnace slags, *Metall. Mater. Trans. B*, 2006, vol. 37 (6), pp. 941-47.

4. H. Hayakawa, M. Hasegawa, K. Oh-nuki, T. Sawai and M. Iwase: Sulphide capacities of CaO-SiO_2-Al_2O_3-MgO slags, *Steel Res. Int.*, 2006, vol. 77 (1), pp. 14-20.

5. S. Ban-Ya: Sulphide capacity and sulphur solubility in CaO-Al_2O_3 and CaO-Al_2O_3 CaF_2 slags, *ISIJ Int.,* 2004, vol. 44 (11), pp. 1810-16.

6. J. D. Seo and S. H. Kim: The sulphide capacity of CaO-SiO_2-Al_2O_3-MgO(-FeO) smelting reduction slags, *Steel Res. ,* 1999, vol. 70 (6), pp. 203-08.

7. M. Nzotta, D. Sichen and S. Seetharaman: A study of the sulfide capacities of iron-oxide containing slags, *Metall. Mater. Trans. B*, 1999, vol. 30 (5), pp. 909-20

8. S. Banya, M. Hino, A. Sato and O. Terayama: Oxygen, phosphorus, and sulfur distribution equilibria between liquid iron and calcium oxide-alumina-iron oxide slag saturated with calcia, *Tetsu-to-Hagane*, 1991, vol. 77 pp. 361-8.

9. T. Tsao: Sulphur distribution between liquid iron and CaO-MgO-Al_2O_3 -SiO_2 slags used for ladle refining, *Trans. Iron Steel Inst. Jpn.,* 1986, vol. 26 (8), pp. 717-23.

10. G. Kor and F. Richardson: Sulfur in lime-alumina mixtures, *J. Iron Steel Inst.,* 1968, vol. 206, pp. 700–04.

11. H. Y. Sohn, M. E. Choi, Y. Zhang and J. E. Ramos: Suspension reduction technology for ironmaking with low CO_2 emission and energy requirement, *Iron Steel Tech. (AIST Trans.),* 2009, vol. 6 (8), pp. 158-65.

12. C. Fincham and F. Richardson: The behaviour of sulphur in silicate and aluminate melts, *Proc. R. Soc. Lond. A,* 1954, vol. 223, pp. 40-62.

13. F. D. Richardson: *Physical Chemistry of Melts in Metallurgy*, Academic Press UK, 1974, vol. 2.

14. K. Karsrud: Alkali capacities of synthetic blast furnace slags at 1500 °C, *Scand. J. Metall.,* 1984, vol. 13 (2), pp. 98-106.

15. R. Young, J. Duffy, G. Hassall and Z. Xu: Use of optical basicity concept for determining phosphorus and sulphur slag-metal partitions, *Ironmaking Steelmaking*, 1992, vol. 19 (3), pp. 201-19.

16. M. M. Nzotta, R. Nilsson, D. Sichen and S. Seetharaman: Sulfide capacities in $MgO-SiO_2$ and $CaO-MgO-SiO_2$ slags, *Ironmaking Steelmaking*, 1997, vol. 24 (4), pp. 300-05.

17. E. F. Osborn, R. C. DeVries, K. H. Gee and H. M. Kraner: Optimum composition of blast-furnace slag as deduced from liquidus data for the quaternary system $CaO-MgO-Al_2O_3-SiO_2$, *J. Met.*, 1954, vol. 6, pp. 33-45.

18. J. Seo and S. Kim: The sulphide capacity of $CaO-SiO_2-Al_2O_3-MgO$ (-FeO) smelting reduction slags, *Steel Res,* 1999, vol. 70 (6), pp. 203-08.

19. J. J. Pak and R. J. Fruehan: Soda slag system for hot metal dephosphorization, *Metall. Trans. B*, 1986, vol. 17B, pp. 797-804.

20. S. Basu, A. Lahiri and S. Seetharaman: Phosphorus partition between liquid steel and $CaO-SiO_2-P_2O_5-MgO$ slag containing low FeO, *Metall. Mater. Trans. B*, 2007, vol. 38 (3), pp. 357-66.

21. J. Brandberg, L. Yu and D. Sichen: Water capacity model of $Al_2O_3-CaO-MgO-SiO_2$ quaternary slag system, *Steel Res.,* 2007, vol. 78 (6), pp. 460-64.

22. M. Nzotta, D. Sichen and S. Seetharaman: Sulphide capacities in some multi component slag systems Sulphide capacities in some multi component slag systems Sulphide capacities in some multi component slag systems, *ISIJ intl.*, 1998, vol. 38 (11), pp. 1170-79.

23. R. Nilsson, M. M. Nzotta, D. Sichen and S. Seetharaman: Determination of the sulfide capacities of multicomponent slag systems by gas/slag equilibration method, *5th Int. Conf. on Molten Slags, Fluxes and Salts,* 1997, pp. 177-90.

24. D. J. Sosinsky and I. Sommerville: The composition and temperature dependence of the sulfide capacity of metallurgical slags, *Metall. Mater. Trans. B*, 1986, vol. 17 (2), pp. 331-37.

25. A. Shankar: Sulphur partition between hot metal and high alumina blast furnace slag, *Ironmaking Steelmaking*, 2006, vol. 33 (5), pp. 413-18.

26. Y. Zhang: Bench-scale flash reduction on iron ore concentrate, *M.S. Thesis*, University of Utah, Salt Lake City, 2008.

27. H. S. Valia: Coke production for blast furnace ironmaking, *http://www.accci.org/Steel.pdf,* (accessed 04/12/2011).

CHAPTER 2

PHOSPHORUS DISTRIBUTION BETWEEN LIQUID IRON AND MAGNESIA-SATURATED SLAG IN H_2/H_2O ATMOSPHERE RELEVANT TO A NOVEL GREEN IRONMAKING TECHNOLOGY

2. 1. Introduction

Reducing phosphorus content in the steel is one of the critical factors to enhance the steel properties. Since the 1940s, researchers have worked on the distribution of phosphorus between hot metal or steel and slag.[1-51] These researchers used Ar, [15-19, 27, 41, 44, 46, 50-51] Ar-CO mixture,[11-12, 26] CO,[31] CO/CO_2,[13] or N_2/CO[14]. Some others worked on the thermodynamics and modeling approaches.[2-11]

As an integral part of a research project which aimed to develop a novel green ironmaking process based on the direct gaseous reduction of iron oxide concentrates in a suspension reduction process, with the ultimate goal of significantly reducing CO_2 emission, energy consumption, and environmental pollution in the steel industry,[52] this research was conducted. Due to the fact that there is no research done to study phosphorus distribution under H_2/H_2O atmosphere p_{O_2}, this research was carried out. A comparison of phosphorus distribution ratio, L_P, between the typical operating conditions of the blast furnace to the proposed green process was carried out.

In this study, equilibrium was established between liquid metal and slag which can be expressed as:

$$[P]+\frac{5}{2}[O]+\frac{3}{2}(O^{2-})=(PO_4^{3-}) \quad (1)$$

where [ ] and ( ) represent species in metal and slag , respectively.

The phosphorus distribution ratio, L_P, between slag and metal can be defined as:

$$L_P=\frac{(\%P)}{[\%P]}=\frac{0.4364\cdot(\%P_2O_5)}{[\%P]} \quad (2)$$

where $(\%P)$= wt% of phosphorus dissolved in slag and $[\%P]$ = wt% of phosphorus dissolved in metal.

The slag basicity was expressed as:

$$B=\frac{(wt\%\,CaO)}{(wt\%\,SiO_2)} \quad (3)$$

2. 2. Experimental Details

The phosphorus experiments were done combined with sulfur experiments in Chapter 1. Thus, all the experimental details were the same.

Metallic iron was analyzed for phosphorus by ICP-OES as well as the entire slag composition. Prior to analysis, the samples were digested in closed Savillex® microwavable vessels. The chemical analysis results are listed in Table 2-1.

In previous research, 6[26] and 8[46] hours were found to be sufficient for a similar sample size. To assure 3-phase (gas-slag-metal) equilibrium, 10 hours was chosen in this work.

Table 2-2 lists the oxygen and sulfur partial pressures for the H_2-H_2O-SO_2 gas mixture at the experimental temperatures were calculated by HSC 5.11 (Outokumpu Oyj, Riihitontuntie 7, Finland), where 15 corresponding gaseous species were taken into consideration.

Comparing our gas rate/ reactor volume to the previous work,[26, 46, 56-62] it was found that this ratio in our system is smaller. Thus, we could also assume that gases are in equilibrium with each other as well as with the condensed phases.

Reproducibility of the experiments was confirmed by the consistency of the results of repeated experiments under the same conditions, as shown Figure 2-1.

2. 3. Results and Discussion

The effect of basicity, oxygen potential, and temperature on phosphorus distribution ratio will be discussed. Also, the blast furnace will be compared to the proposed process for L_P. Considering the difficulty of the direct comparison of our results to the previous results, in addition to the fact that the available theoretical models[3-5, 10] did not consider the H_2 and H_2O interaction with the slag, it was difficult to get results predicted by these models of reasonable agreement with the experimental results. From previous research,[63] water has a significant solubility in slag, indicating that it could affect the L_P. It was found that further theoretical study is needed to develop a model to predict the L_P under H_2/H_2O atmosphere.

Table 2-1. The chemical analysis of the samples.

Sample	(P)%	FeO%	MgO%	CaO%	Al_2O_3%	SiO_2%	[P]%	T^0C	L_P
S1	0.0602	25.3	17.3	20.7	6.26	29.8	0.00653	1550	9.21
S2	0.0953	35.4	12.9	20.6	6.72	24.6	0.00587	1550	16.2
S3	0.130	33.1	11.7	26.3	7.81	28.5	0.00682	1550	19.1
S4	0.112	41.3	10.8	21.5	6.20	21.0	0.00532	1550	21.0
S5	0.109	21.6	19.2	20.9	8.74	28.3	0.00645	1550	17.0
S6	0.107	19.9	20.2	23.0	7.99	33.0	0.00662	1550	16.0
S7	0.0965	22.3	15.2	29.8	9.48	26.4	0.00753	1550	12.8
S8	0.143	20.7	10.6	32.1	9.35	23.7	0.00640	1550	22.3
S9	0.119	11.5	22.4	24.9	8.18	32.3	0.0105	1550	11.3
S10	0.156	12.0	18.7	29.0	9.71	29.9	0.00880	1550	17.6
S11	0.0865	12.4	17.0	30.9	10.7	29.0	0.00779	1550	11.1
S12	0.129	14.2	14.5	34.7	9.82	31.0	0.00715	1550	18.1
S13	0.123	12.2	22.5	25.1	9.41	32.6	0.0106	1550	11.6
S14	0.137	12.6	16.9	27.4	8.77	39.7	0.00808	1550	16.9
S15	0.123	18.7	15.4	34.7	10.23	16.4	0.00628	1550	19.6
S16	0.132	15.3	16.3	32.4	10.4	28.4	0.00577	1550	22.8
S17	0.0238	41.1	15.1	15.8	6.15	19.5	0.00742	1600	3.21
S18	0.0627	34.6	13.6	20.4	7.37	24.4	0.00619	1600	10.1
S19	0.0802	42.8	11.3	18.1	6.25	17.0	0.00601	1600	13.3

Table 2-1. Continued.

Sample	(P)%	FeO%	MgO%	CaO%	Al_2O_3%	SiO_2%	[P]%	T^0C	L_P
S20	0.0577	52.8	12.4	14.9	4.90	12.3	0.00522	1600	11.0
S21	0.0526	20.4	22.6	20.7	7.55	27.7	0.00672	1600	7.83
S21	0.0438	20.3	22.6	20.7	8.63	27.6	0.00743	1600	5.90
S22	0.0790	27.1	15.7	22.7	8.24	23.5	0.00660	1600	12.0
S22	0.0876	27.0	17.6	22.6	8.23	23.2	0.00575	1600	15.2
S23	0.0828	29.7	14.2	26.2	8.77	22.0	0.00645	1600	12.8
S23	0.0826	29.7	14.2	23.7	8.34	22.0	0.00469	1600	17.6
S24	0.0251	31.1	14.7	24.9	7.93	21.7	0.00610	1600	4.12
S25	0.0752	8.70	25.5	24.3	9.71	36.0	0.0255	1600	2.95
S26	0.0527	9.31	21.2	27.1	9.83	31.5	0.0206	1600	2.56
S27	0.0815	11.8	18.7	29.1	10.1	28.2	0.0177	1600	4.61
S28	0.0903	13.2	19.4	31.0	9.89	23.9	0.0132	1600	6.85
S29	0.0765	7.12	23.9	23.9	9.62	31.5	0.0136	1600	5.61
S30	0.0740	14.7	20.9	25.5	9.55	28.2	0.0108	1600	6.85
S31	0.0853	14.9	25.3	25.2	8.90	23.6	0.00869	1600	9.81
S37	0.0652	32.6	20.6	17.8	7.62	23.5	0.0105	1650	6.21
S38	0.0715	47.5	14.2	13.5	5.52	16.3	0.00943	1650	7.58

Table 2-2. Oxygen and sulfur partial pressures calculated at the experimental temperatures.

(1 atm = 101.325 kPa)

H_2/ H_2O (molar ratio)	p_{O_2} (atm)			p_{S_2} (atm)			Flow Rates (mL/min)		
	1550ºC	1600ºC	1650ºC	1550ºC	1600ºC	1650ºC	H_2	H_2O	SO_2
1.7	2.2×10^{-09}	4.8×10^{-09}	-	1.4×10^{-03}	1.7×10^{-03}	-	125	0.047	5.7
3.0	7.0×10^{-10}	1.8×10^{-09}	4.2×10^{-09}	1.0×10^{-03}	1.3×10^{-03}	1.6×10^{-03}	149	0.032	5.7
6.0	2.4×10^{-10}	5.3×10^{-10}	-	8.3×10^{-04}	1.0×10^{-03}	-	170	0.018	5.7
10.0	1.1×10^{-10}	2.7×10^{-10}	-	7.3×10^{-04}	9.5×10^{-04}	-	181	0.011	5.7

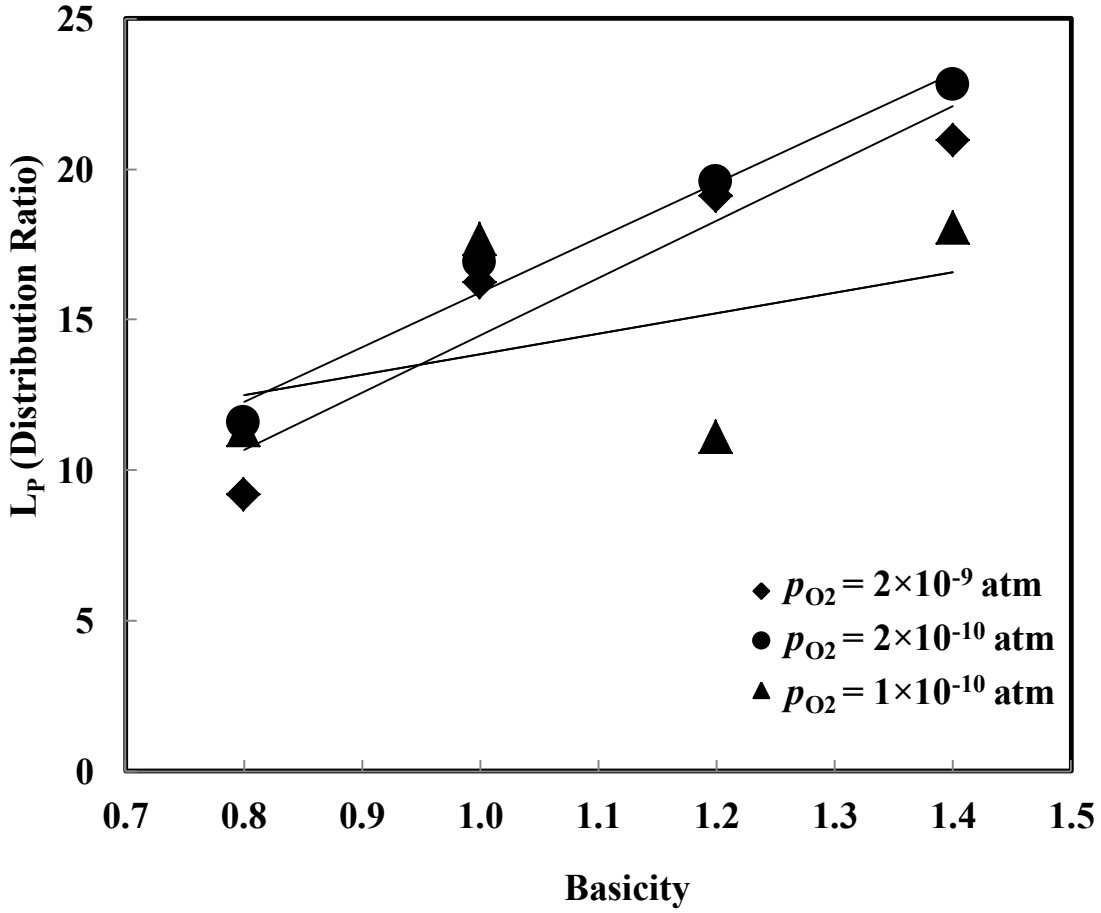

Figure 2-1. The effect of basicity on L_p at 1550^0C and different gas compositions.

2. 3. 1. Effect of Basicity

The effect of basicity on the phosphorus partition is shown in Figures 2-1 – 2-3 which indicate that the higher the basicity, the higher the L_P was as expected from thermodynamics since oxygen activity increases with basicity. As a result, L_P increased according to reaction (1). This is the same trend as determined in the previous research[12, 30, 44, 46, 49,64] in this range of basicity; 0.8-1.2. In addition to water vapor effect, slag composition, and p_{O_2} were also different from the present conditions; it was difficult to directly compare the results to previous results.

2. 3. 2. Effect of Oxygen Potential

The previous work[1-51] was done under oxygen potential lower than 10^{-9} and it was found that L_P increases with oxygen potential. In the current work, a wider range of oxygen potentials was studied. It was found that at 1600°C, the trend was similar to the previous investigations when oxygen potential was lower than 10^{-9}. At p_{O_2} higher than this value, there was a reversal in the trend: L_P started to decrease with the increasing p_{O_2}, as shown in Figures 2-4 – 2-7.

At 1550°C and basicity lower than 1.2, L_P slightly changed with Log p_{O_2} until p_{O_2} reached approximately 10^{-9}, L_P either decreased, when basicity was 0.8, as shown in Figure 2-4, or stayed constant when basicity was 1.0, as shown in Figure 2-5. While at the same temperature but higher basicities, 1.2 and 1.4, L_P showed a similar trend as at 1600°C.

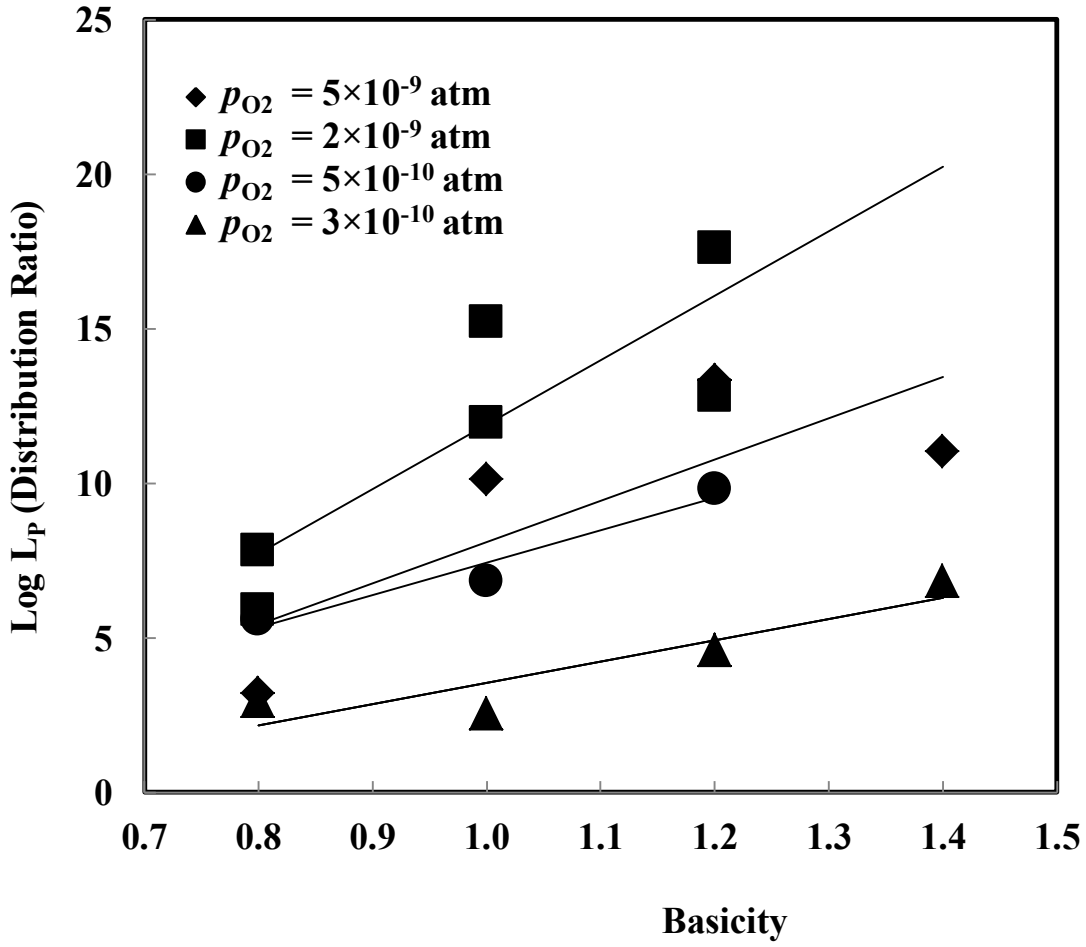

Figure 2-2. The effect of basicity on L_p at 1600°C and different gas compositions.

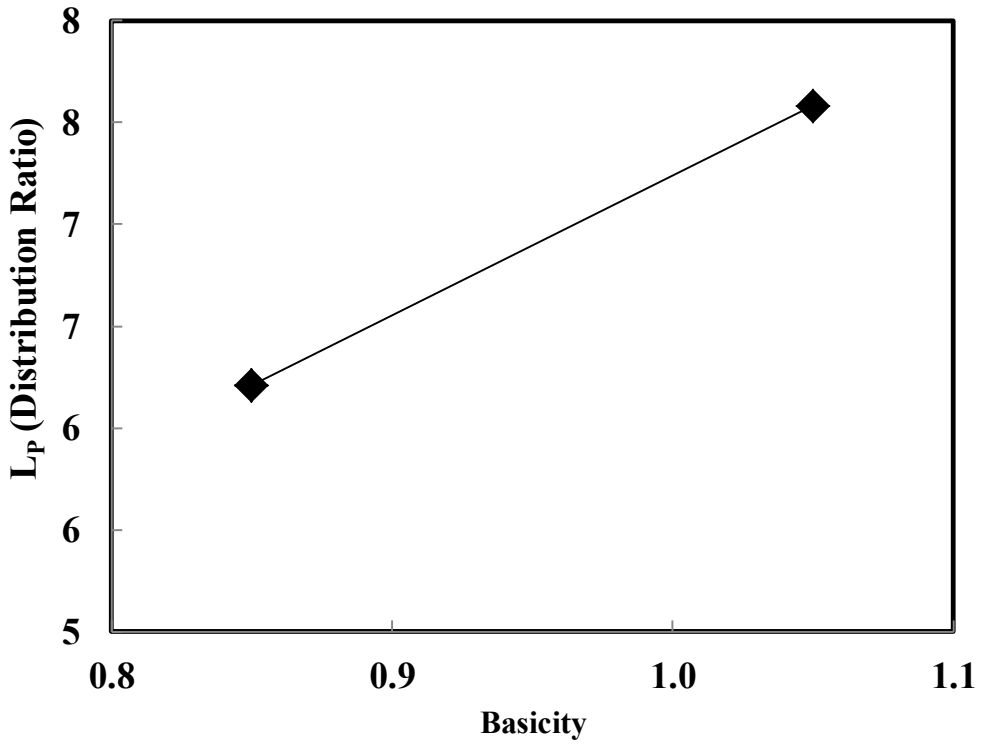

Figure 2-3. The effect of basicity on L_P at 1650°C and $p_{O_2} = 4\times10^{-9}$ atm.

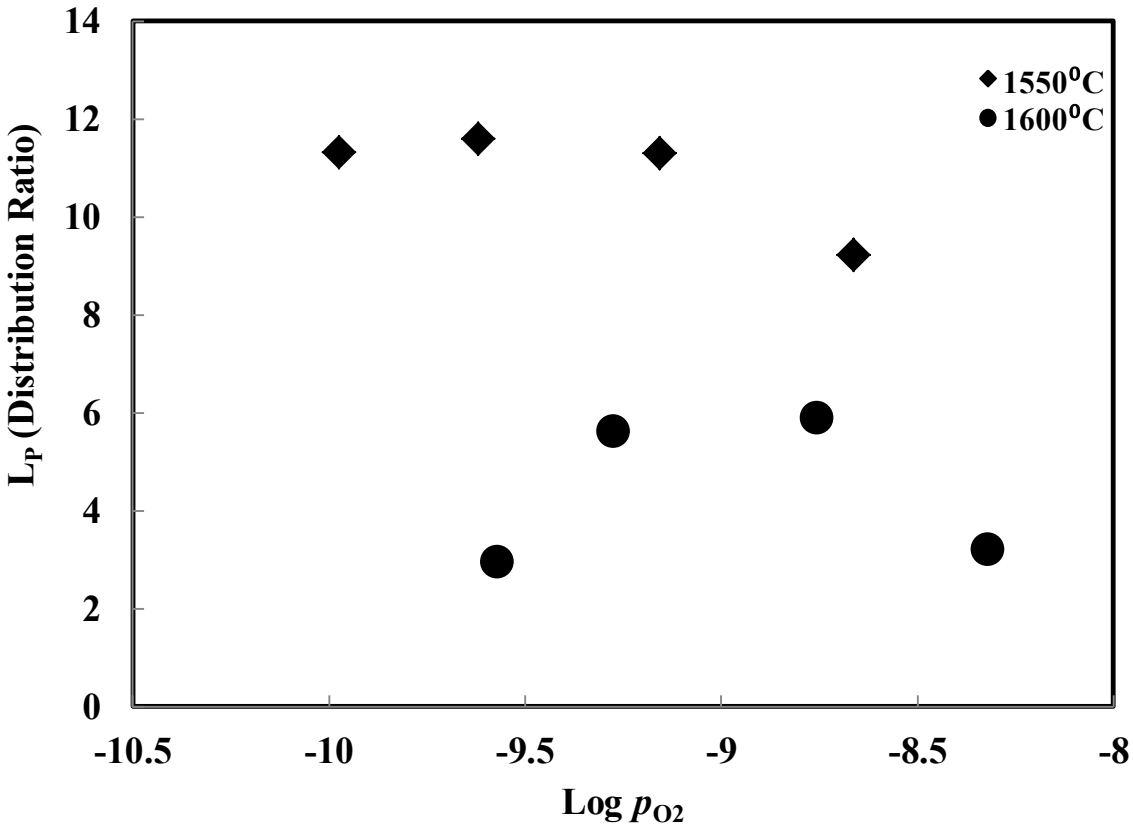

Figure 2-4. The effect of oxygen potential on L_P at basicity of 0.8 at 1550°C and 1600°C.

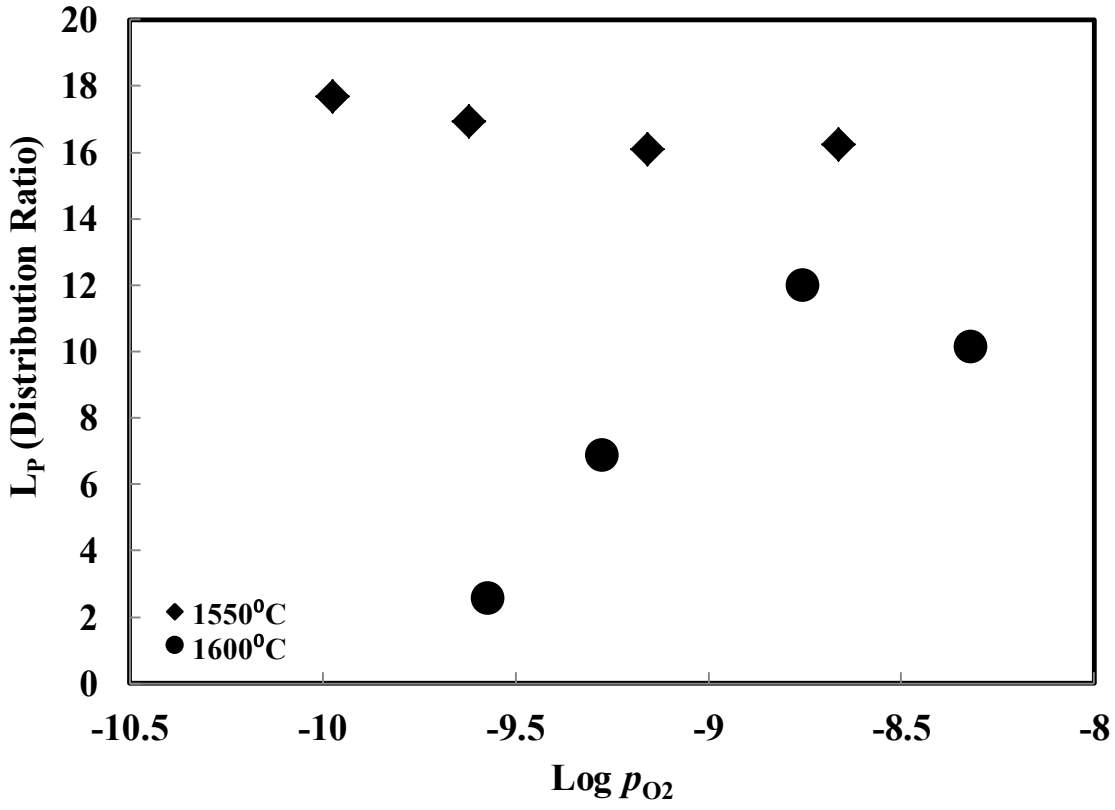

Figure 2-5. The effect of oxygen potential on L_P at basicity of 1 at 1550°C and 1600°C.

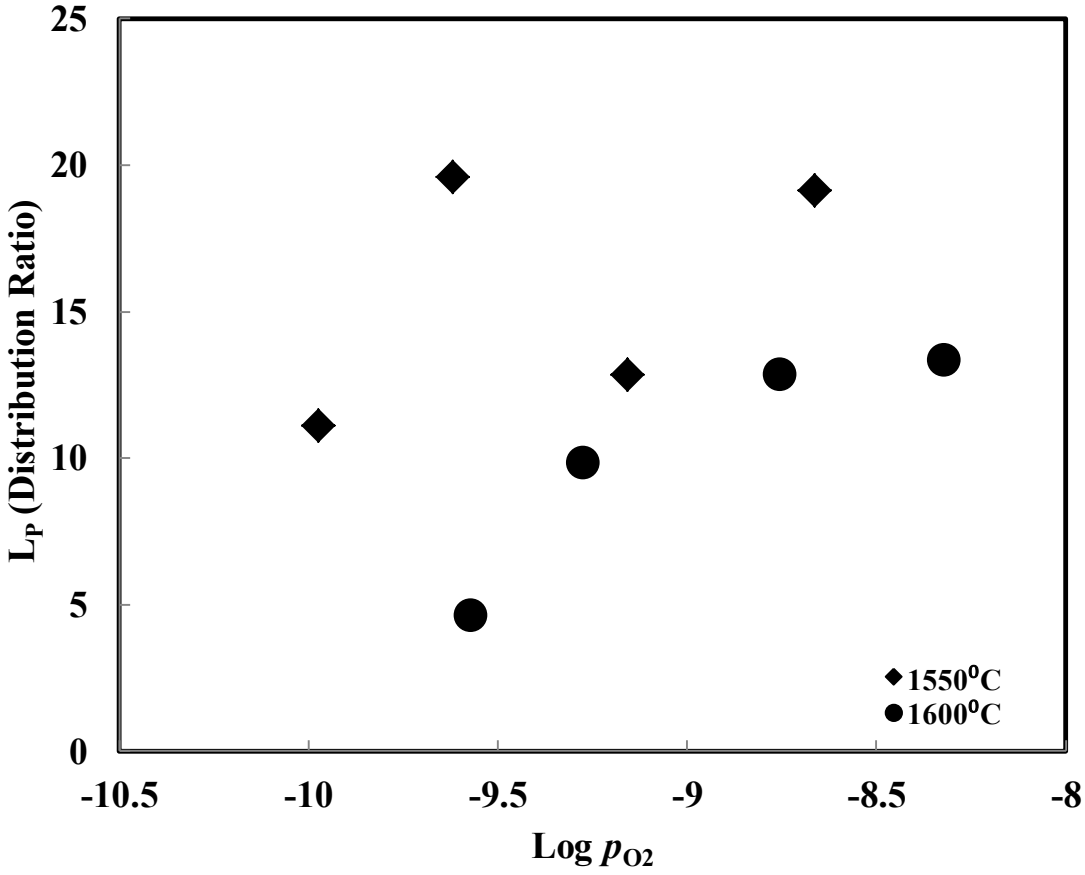

Figure 2-6. The effect of oxygen potential on L_P at basicity of 1.2 at 1550^{0}C and 1600^{0}C.

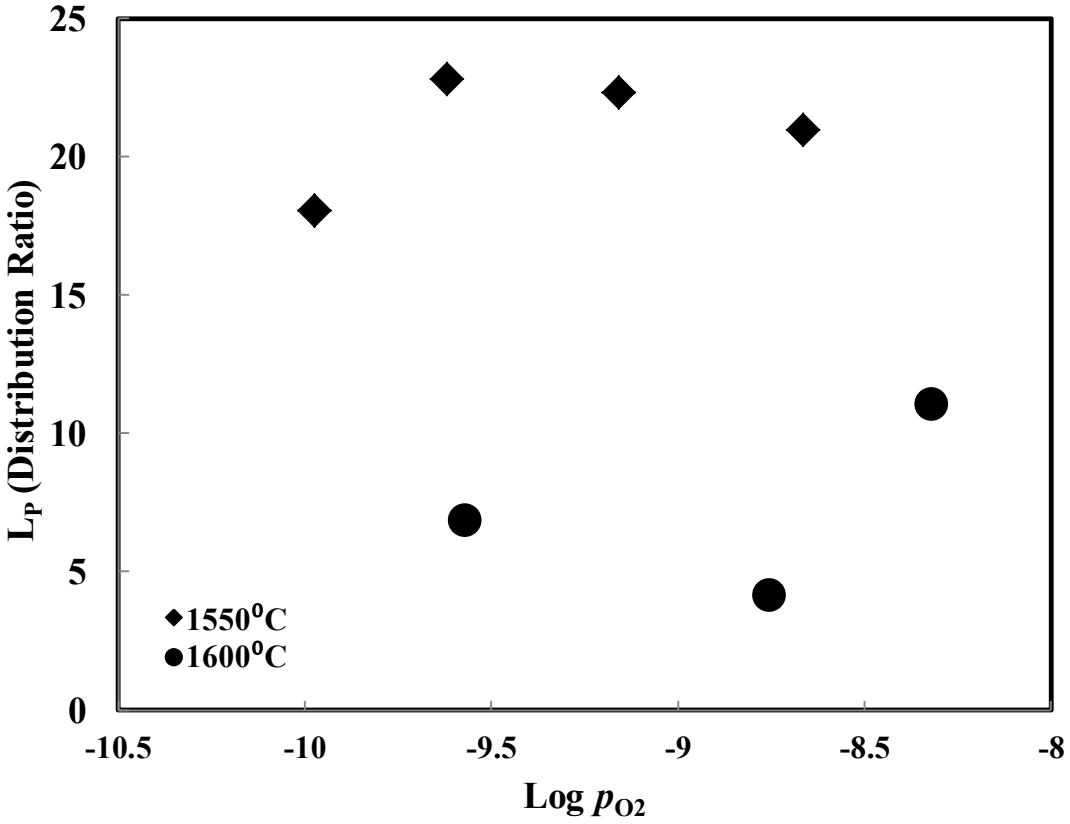

Figure 2-7. The effect of oxygen potential on L_P at basicity of 1.4 at 1550 °C.

Basu *et al.*[48] reported a similar trend at 1600 and 1650°C when FeO reached 15-20 wt%. L_P increased with FeO content until the latter reached 15-20 wt%, and a maximum in the distribution ratio was reached. Then a reversal occurred where L_P decreased with increasing FeO content, as shown in Figure 2-8.

This behavior can be attributed to the variation of the activity coefficient of P_2O_5 ($\gamma_{P_2O_5}$) with respect to FeO content. The same authors found that $\gamma_{P_2O_5}$ decreased with increasing FeO at FeO content less than 20-30 wt%: Beyond that value, $\gamma_{P_2O_5}$ started to increase.

2. 3. 3. Effect of Temperature

It is shown in Figure 2-9 that L_P decreased with increasing temperature at constant input gas composition and basicity which was consistent with the previously reported results.[31, 44, 46, 49] This should be explained by the fact that P goes to slag as P_2O_5 which is an exothermic process.

2. 3. 4. Blast Furnace Versus the Proposed Green Ironmaking Technology

Shankar[65] reported blast furnace data from the G furnace of Tata Steel. Also, Young *et al*.[4] listed the composition of the blast furnace typical slag. Combining the information from these authors, L_P was approximately 0.02. While in the proposed process, L_P was in the range of 9-21 at and of 2.2×10-09 and 1.4×10-03, respectively, and the temperature of 1550°C (samples 1-4 in Table 2-2). These conditions are the closest to the optimum conditions of the proposed process. Also, one major difference between the blast furnace slag and the proposed process slag is the total iron which is < 4

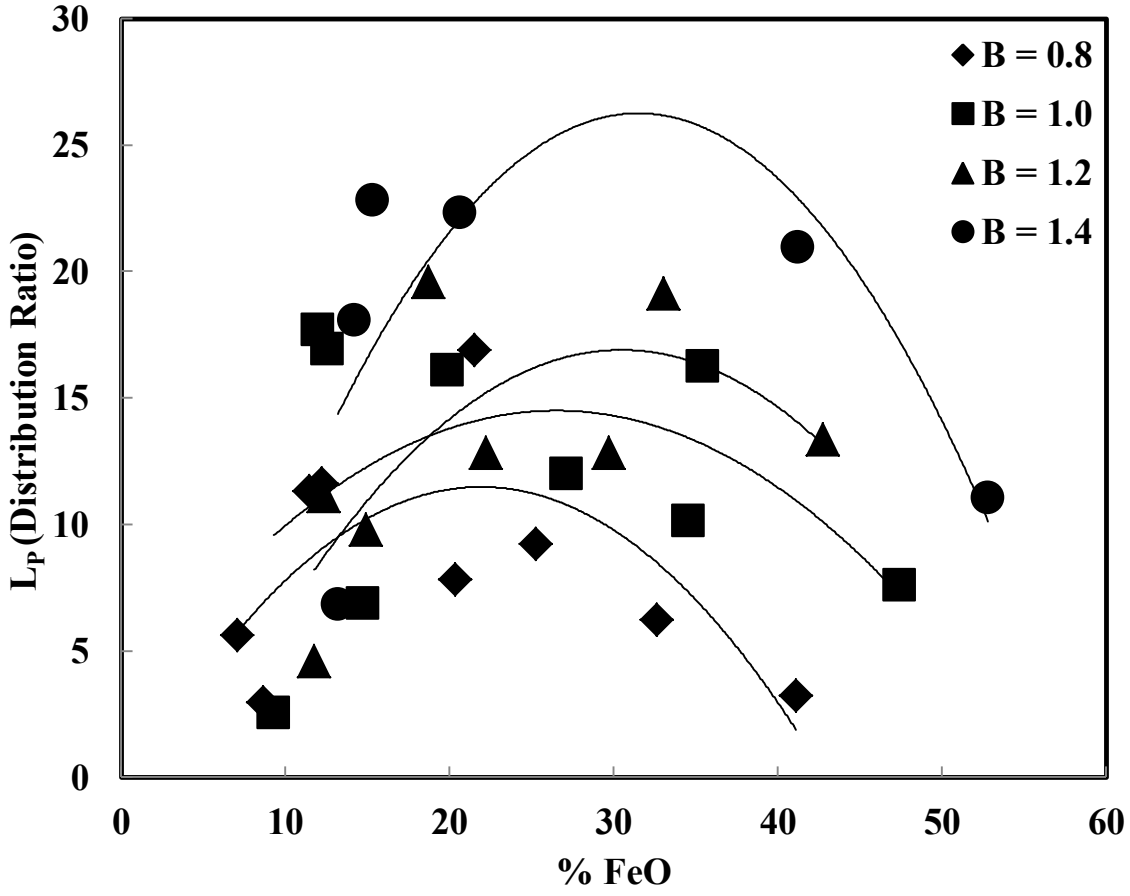

Figure 2-8. The effect of FeO content on L_P at different basicities with a second-order polynomial trend.

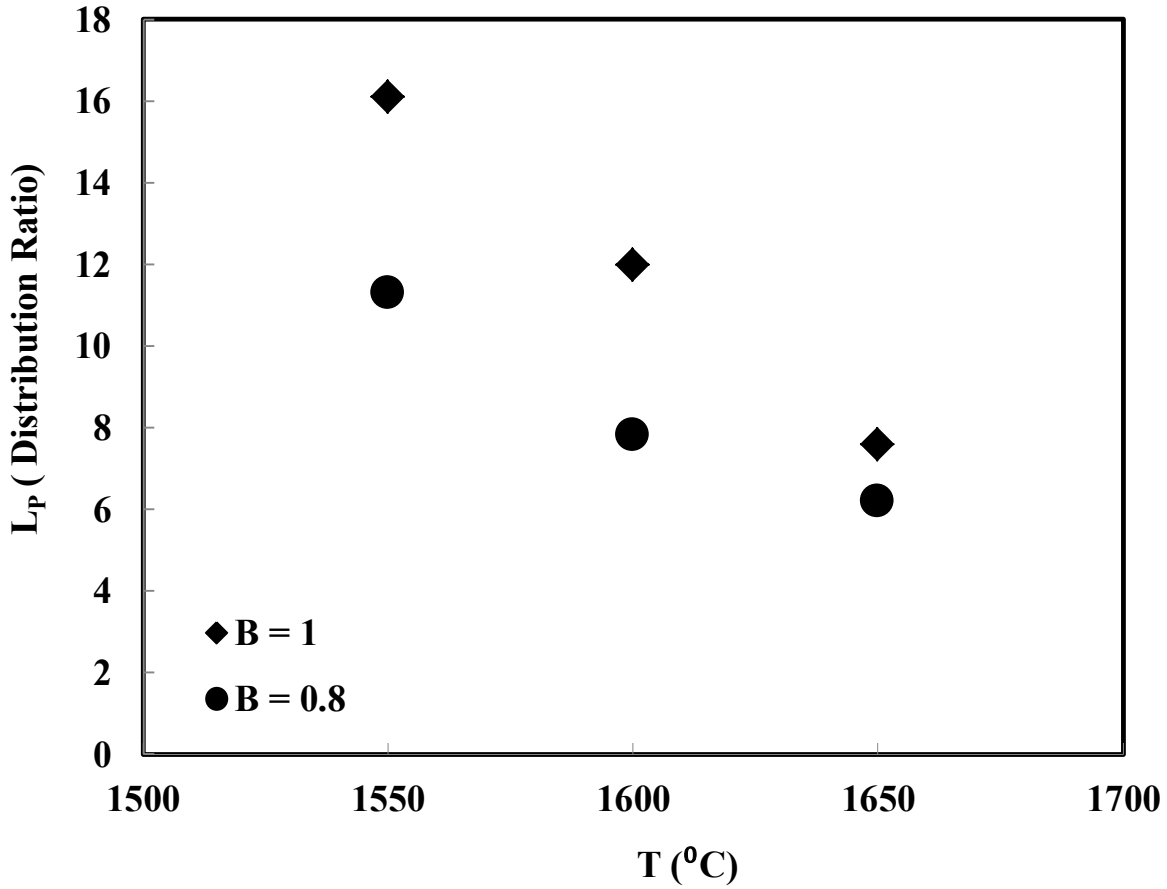

Figure 2-9. The effect of temperature on L_P at H_2/H_2O = 3 and basicity = 1, 0.8.

wt% in the blast furnace slag and 26-43 wt% in samples 1-4. This means in the proposed process, the L_P is 450-1050 times that in the blast furnace. Also considering the amount of phosphorus input in the two processes where the proposed process has phosphorus of approximately 0.01 wt%[66] of ore weight, while in the blast furnace, the coke is another source of phosphorus. Coke has phosphorus average of 0.02 wt%.[67] This means that the phosphorus input in the blast furnace is approximately three times that in the proposed process. Thus, the proposed process is expected to produce hot metal with much lower phosphorus which will minimize the need for dephophorization in the steelmaking step.

2. 4. Conclusions

In the present work, the phosphorus distribution ratio (L_P) between molten iron and $CaO\text{-}MgO_{(Saturated)}\text{-}SiO_2\text{-}Al_2O_3\text{-}FeO$ slag was determined in the temperature range 1550-1650°C. Oxygen partial pressure was controlled by H_2/H_2O equilibrium in the range of 10^{-8}-10^{-10} atm. It was found that the trend of the distribution was similar to the previous work for the dependence on basicity and temperature, while the response to the oxygen partial pressure was studied for the first time and showed different behavior.

In the proposed process, L_P was found 450-1050 times that of the blast furnace. Also, considering the amount of phosphorus input in the two processes, it was found that L_P of the blast furnace is approximately three times that of the proposed process. This means that the proposed process will produce hot metal with much lower phosphorus which will minimize the need to dephophorization. For the future work, further study should be carried to study the impact of H_2 and H_2O on L_P.

2. 5. References

1. A. Bergman and A. Gustafsson: On the relation between optical basicity and phosphorus capacity of complex slags, *Steel Res.,* 1988, vol. 59 (7), pp. 281-88.

2. B. Deo, P. Bose and K. Mehrotra: Models for predicting phosphorus and sulphur distribution ratios in oxygen steel making *, Trans. Indian Inst. Met.,* 1988, vol. 41 (5), pp. 475-79.

3. R. Young, J. Duffy, G. Hassall and Z. Xu: Use of optical basicity concept for determining phosphorus and sulphur slag-metal partitions, *Ironmaking Steelmaking,* 1992, vol. 19 (3), pp. 201-19.

4. V. Novikov, V. Nevidimov and G. Toporishchev: Application of polymeric model for the calculation of phosphorus distribution between metal and slag, *Rasplavy(Russia),* 1995, vol. 6, pp. 72-74.

5. X. Yang, T. Liu, Z. Guo and D. Wang: Study on the correlation between phosphate capacity index and slag basicity, In *Selected Papers of Engineering Chemistry and Metallurgy,* Science Press, China, 1996, vol. 8, pp. 8-21.

6. K. Ide and R. J. Fruehan: Evaluation of phosphorus reaction equilibrium in steelmaking, *Iron Steelmaker,* 2000, vol. 27, pp. 65-70.

7. M. Hasegawa, M. Iwase, K. Wakimoto and A. McLean: A thermochemical study of the CaO + P2O5 + FexO system-regions in equilibrium with solid $Ca_3P_2O_8$, *Scand. J. Metall.,* 2002, vol. 32, pp. 47-52.

8. G. Li, T. Hamano and F. Tsukihashi: Thermodynamics of dephosphorization of molten steel by MgO saturated CaO-Fe_tO-SiO_2-Na_2O, Al_2O_3 fluxes, *Proc. of the Int. Congress on the Science and Technology of Steelmaking*, Association for Iron & Steel Technology, New York, 2005, pp. 125-30.

9. S. Basu, A. Lahiri and S. Seetharaman: A model for activity coefficient of P_2O_5 in BOF slag and phosphorus distribution between liquid steel and slag, *ISIJ Int.,* 2007, vol. 47 (8), pp. 1236-38.

10. A. H. Chan, J. J. Pak and R. J. Fruehan: The thermodynamics of sulfur and phosphorus reacting between carbon-saturated iron and sodium oxide-silicon dioxide slags, *Proc. Process Technol. Conf.*, USA, 1986, pp. 467-73.

11. B. Maramba and R. Eric: Phosphide capacities of ferromanganese smelting slags, *Miner. Eng.,* 2008, vol. 21 (2), pp. 132-37.
12. E. Turkdogan and P. Bills: Thermodynamic study of Fe-Ca-P-O, Fe-Ca-Si-P-O, and some complex molten silicophosphate systems, *Iron and Steel Inst.,* London, 1958, vol. 188, pp. 143-53.

13. H. Knuppel, F. Oeters: Das Phosphor-Sauerstoff-Gleichgewicht zwischen flüssigem Eisen und kalkgesättigten Phosphatschlacken (The phosphorus-oxygen equilibrium between liquid iron and lime saturated phosphate slag), *Stahl Eisen,* 1961, vol. 81 (22), pp. 1437-49.

14. H. Suito and R. Inoue: Effects of sodium oxide and barium oxide additions on phosphorus partition between calcium oxide-magnesium oxide-iron oxide (FeO)-silicon dioxide slags and molten iron , *Trans. Iron Steel Inst. Jpn.,* 1984, vol. 24, pp. 47-53.

15. H. Suito and R. Inoue: Manganese equilibrium between molten iron and MgO-Saturated CaO-Fe_tO-SiO_2-MnO Slags, *Trans. Iron Steel Inst. Jpn.,* 1984, vol. 24 (4), pp. 257-65.

16. H. Suito, R. Inoue and M. Takada: Phosphorus distribution between liquid iron and MgO saturated slags of the system CaO-MgO-FeO_x-SiO_2, *Trans. Iron Steel Inst. Jpn.,* 1981, vol. 21 (4), pp. 250-59.

17. Y. Kawai, R. Nakao and K. Mori: Dephosphorization of liquid iron by CaF_2-base fluxes, *Trans. Iron Steel Inst. Jpn.,* 1984, vol. 24 (7), pp. 509-14.

18. K. Kunisada and H. Iwai: Phosphorus distribution between liquid iron and slags of sodium oxide-silica-iron oxide (Na_2O-SiO_2-Fe_tO) system, *Proc. Process Technol. Conf.*, Iron Steel Tech. Coll., USA, 1986, pp. 419-23.

19. I. A. Tomilin and L. A. Shvartsman: Distribution of sulfur and phosphorus between iron and acid slag, *Probl. Metallography Physics Metals,* 1959, vol., pp. 418-24.

20. K. Koch, T. Kootz and H. D. Pflipsen: Distribution of sulphur, phosphorus and manganese between the final slag and molten steel in large LD converters, *Arch. Eisenhuttenwes.,* 1981, vol. 52 (3), pp. 103-07.

21. R. Inoue and H. Suito: Phosphorus distribution between soda- and lime-based fluxes and carbon-saturated iron melts, *Tetsu-to-Hagane(J. Iron Steel Inst. Jpn.),* 1985, vol. 71 (2), pp. 212-19.

22. K. Kunisada: Effects of CaO and MgO on the phosphorus distribution between liquid iron and slags of Na_2O-SiO_2 systems, *Trans. Iron Steel Inst. Jpn.,* 1985, vol. 25 (12), p. B349.

23. Y. Shirota, K. Katohgi, K. Klein, H. J. Engell and D. Janke: Phosphate capacity of FeO-Fe_2O_3-CaO-P_2O_5 and FeO-Fe_2O_3-CaO-CaF_2-P_2O_5 slags by levitation melting, *Trans. Iron Steel Inst. Jpn.,* 1985, vol. 25 (11), pp. 1132-40.

24. S. Simeonov and N. Sano: Phosphorus equilibrium distribution between slags containing MnO, BaO and Na_2O carbon-saturated iron for hot metal pretreatment, *Trans. Iron Steel Inst. Jpn.,* 1985, vol. 25 (10), pp. 1031-35.

25. J. J. Pak and R. J. Fruehan: Soda slag system for hot metal dephosphorization, *Metall. Mater. Trans. B,* 1986, vol. 17B, pp. 797-04.

26. K. Kunisada and H. Iwai: Effect of Na_2O in phosphorus distribution between liquid iron and CaO-based slags *,Trans. Iron Steel Inst. Jpn.,* 1987, vol. 27 (4), pp. 263-69.

27. K. Kunisada and H. Iwai: Effects of CaO, MnO, and Al_2O_3 on phosphorus distribution between liquid iron and Na_2O-MgO-Fe_tO-SiO_2 slags, *Trans. Iron Steel Inst. Jpn.,* 1987, vol. 27 (5), pp. 332-39.

28. A. Werme and P. Lundh: Distribution of phosphorus between some CaO-FeO-SiO_2-P_2O_5 (10%) slags and carbon-saturated liquid iron at 1300°C, *Scand. J. Metall.,* 1987, vol. 16 (1), pp. 33-41.

29. R. Selin, Y. Dong and Q. Wu: Uses of lime-based fluxes for simultaneous removal of phosphorus and sulphur in hot metal pretreatment, *Scand. J. Metall.,* 1990, vol. 19 (3), pp. 98-09.

30. N. F. Ahundov, F. Tsukihashi and N. Sano: Equilibrium partitions of manganese and phosphorus between barium oxide-barium fluoride melts and carbon saturated iron-manganese melts, *ISIJ Int.,* 1991, vol. 31, pp. 685-88.

31. S. Banya, M. Hino, A. Sato and O. Terayama: Oxygen, phosphorus, and sulfur distribution equilibria between liquid iron and calcium oxide-alumina-iron oxide slag saturated with calcia, *Tetsu-to-Hagane,* 1991, vol. 77 pp. 361-68.

32. C. Nassaralla and R. Fruehan: Phosphate capacity of CaO-Al_2O_3 slags containing CaF_2, BaO, Li_2O, or Na_2O, *Metall. Mater. Trans. B,* 1992, vol. 23 (2), pp. 117-23.

33. O. Ostrovski, Y. Utoshkin, A. Pavlov and R. Akberdin: Phosphate capacity of the CaO-CaF_2 system containing chromium oxide, *ISIJ Int.,* 1994, vol. 34 (10), pp. 849-51.

34. H. Ishii and R. J. Fruehan: Dephosphorization equilibria between liquid iron and highly basic CaO-based slags saturated with MgO, *Iron Steelmaker,* 1997, vol. 24, pp. 47-54.

35. J. Borode: Phosphorus partition ratio and phosphate capacity of Na_2O-SiO_2 at 1400°C, *Ironmaking Steelmaking,* 1998, vol. 25 (2), pp. 144-49.

36. E. Kawecka-Cebula: Determination of the phosphorus capacity and phosphor partition coefficient from the chemical composition of slag, *Metall. Foundry Eng.,* 1998, vol. 24, pp. 71-87.

37. W. Van Niekerk and R. Dippenaar: Phosphorus distribution between carbon-saturated iron at 1350°C and lime-based slags containing Na_2O and CaF_2, *Metall. Mater. Trans. B,* 1998, vol. 29 (1), pp. 147-53.

38. B. Grüneberg and J. Kern: Phosphorus retention capacity of iron-ore and blast furnace slag in subsurface flow constructed wetlands, *Water Sci. Technol.,* 2001, vol. 44 (11-12), pp. 69-75.

39. B. Deo, J. Halder, B. Snoeijer, A. Overbosch and R. Boom: Effect of MgO and Al_2O_3 variations in oxygen steelmaking (BOF) slag on slag morphology and phosphorus distribution, *Ironmaking Steelmaking,* 2005, vol. 32 (1), pp. 54-60.

40. C. M. Lee and R. J. Fruehan: Phosphorus equilibrium between hot metal and slag, *Ironmaking Steelmaking,* 2005, vol. 32, pp. 503-08.

41. Q. Wang, J. Zhou, X. Du, Distribution of phosphorus between CaO-CaF_2 slag and Fe-CP Melt, *J. Iron Steel Res. Int.,* 2005, vol. 12 (1), pp. 5-8.

42. H. Saridikmen, C. S. Kucukkaragoz and R. H. Eric: Phosphorus distribution between metal and slag phases pertinent to ferromanganese smelting, *Sohn International Symposium*, San Diego, 2006, pp. 547-58.

43. S. Basu, A. Lahiri and S. Seetharaman: Phosphorus partition between liquid steel and CaO-SiO_2-P_2O_5-MgO slag containing low FeO, *Metall. Mater. Trans. B,* 2007, vol. 38 (3), pp. 357-66.

44. S. Basu, A. Lahiri, S. Seetharaman and J. Halder: Change in phosphorus partition during blowing in a commercial BOF, *ISIJ Int.,* 2007, vol. 47 (5), pp. 766-68.

45. S. Basu, A. K. Lahiri and S. Seetharaman: Phosphorus partition between liquid steel and CaO-SiO_2-FeO_x-P_2O_5-MgO slag containing 15 to 25 pct FeO, *Metall. Mater. Trans. B,* 2007, vol. 38B, pp. 623-30.

46. Q. Lu, F. M. Li, S. H. Zhang and J. M. Huang: Effect of temperature and gas pressure on phosphorus capacity of CaO-SiO_2-Al_2O_2-MgO-Fe_tO system, *Chinese Journal of Nonferrous Metals,* 2007, vol. 17 (11), pp. 1871-75.

47. D. Shin, C. Wee, M. Kim, B. You, J. Han, S. Choi and D. Yun: Distribution behavior of vanadium and phosphorus between slag and molten steel, *Met. Mat. Int.,* 2007, vol. 13 (2), pp. 171-76.

48. S. Basu, A. K. Lahiri and S. Seetharaman: Distribution of phosphorus and oxygen between liquid steel and basic oxygen steelmaking slag, *Rev. Metall.,* 2009, vol. 106, pp. 21-26.

49. K. Mori, T. Kaneko and Y. Kawai: Rate of transfer of phosphorus between metal and slag, *Trans. Iron Steel Inst. Jpn.,* 1978, vol. 18 (5), pp. 261-68.

50. J. C. Wrampelmeyer, S. Dimitrov and D. Janke: dephosphorization equilibria between pure molten Iron and CaO-Saturated FeO_n-CaO-SiO_2 and FeO_n-CaO-Al_2O_3 slags, *Steel Res.,* 1989, vol. 60 (12), pp. 539-49.

51. H. Y. Sohn, M. E. Choi, Y. Zhang and J. E. Ramos: Suspension reduction technology for ironmaking with low CO_2 emission and energy requirement, *Iron Steel Tech.(AIST),* 2009, vol. 6 (8), pp. 158-65.

52. M. M. Nzotta, R. Nilsson, D. Sichen and S. Seetharaman: Sulfide capacities in MgO-SiO_2 and CaO-MgO-SiO_2 slags, *Ironmaking Steelmaking,* 1997, vol. 24 (4), pp. 300-05.

53. E. F. Osborn, R. C. DeVries, K. H. Gee and H. M. Kraner: Optimum composition of blast-furnace slag as deduced from liquidus data for the quaternary system CaO-MgO-Al2O3-SiO2, *J. Met.,* 1954, vol. 6, pp. 33-45.

54. J. Seo and S. Kim: The sulphide capacity of CaO-SiO_2-Al_2O_3-MgO (-FeO) smelting reduction slags, *Steel Res.,* 1999, vol. 70 (6), pp. 203-08.

55. C. Fincham and F. Richardson: The behaviour of sulphur in silicate and aluminate melts, *Proc. R. Soc. Lond. A,* 1954, vol. pp. 40-62.

56. Y. Taniguchi: Sulphide capacities of CaO-Al_2O_3-SiO_2-MgO-MnO slags in the temperature range 1673-1773K, *ISIJ Int.,* 2009, vol. 49 (2), pp. 156-63.

57. A. Shankar, M. Görnerup, S. Seetharaman and A. Lahiri: Sulfide capacity of high alumina blast furnace slags, *Metall. Mater. Trans. B,* 2006, vol. 37 (6), pp. 941-47.

58. H. Hayakawa, M. Hasegawa, K. Oh-nuki, T. Sawai and M. Iwase: Sulphide capacities of CaO-SiO_2-Al_2O_3-MgO slags, *Steel Res. Int.,* 2006, vol. 77 (1), pp. 14-20.

59. S. Ban-Ya: Sulphide capacity and sulphur solubility in CaO-Al_2O_3 and CaO-Al_2O_3 CaF_2 slags, *ISIJ Int.,* 2004, vol. 44 (11), pp. 1810-16.

60. J. D. Seo and S. H. Kim: The sulphide capacity of CaO-SiO_2-Al_2O_3-MgO (-FeO) smelting reduction slags, *Steel Res.,* 1999, vol. 70 (6), pp. 203-08.

61. M. Nzotta, D. Sichen and S. Seetharaman: A study of the sulfide capacities of iron-oxide containing slags, *Metall. Mater. Trans. B,* 1999, vol. 30 (5), pp. 909-20.

62. E. Turkdogan: *Fundamentals of Steelmaking*, The Institute of Materials, London, 1996.

63. J. Brandberg, L. Yu and D. Sichen: Water capacity model of Al_2O_3-CaO-MgO-SiO_2 quaternary slag system, *Steel Res.,* 2007, vol. 78 (6), pp. 460-64.

64. A. Shankar: Sulphur partition between hot metal and high alumina blast furnace slag, *Ironmaking Steelmaking,* 2006, vol. 33 (5), pp. 413-18.

65. Y. Zhang: Bench-scale flash reduction on iron ore concentrate, *M.S.Thesis*, University of Utah, Salt Lake City, 2008, p. 13.

66. H. S. Valia: Coke production for blast furnace ironmaking, *http://www.accci.org/Steel.pdf*, (accessed 04/12/2011).

CHAPTER 3

FUTURE WORK

3. 1. Sulfur Distribution

The thermodynamics of sulfur reactions in the slag need to be studied in order to clearly understand the effect of H_2 and H_2O on the sulfur distribution. Also, experimental work might be conducted to determine the optimum slag composition that will have higher sulfide capacity under H_2/H_2O atmosphere. Moreover, a model that is independent of adjustable parameters but rather with a thermodynamics basis should be developed to interpret the sulfur distribution under H_2/H_2O conditions.

3. 2. Phosphorus Distribution

The thermodynamics of phosphorus reaction in the slag should be studied in order to clearly understand the effect of H_2 and H_2O on the sulfur distribution. Moreover, a model that is independent of adjustable parameters but rather with a thermodynamics basis should be developed to interpret the phosphorus distribution under H_2/H_2O conditions.

3. 3. Other Minor Elements Distribution

Experimental and theoretical work should be conducted in order to investigate the distribution of more minor elements as Mn and Cr under H_2/H_2O atmosphere.

3. 4. Iron Oxide Activity Coefficient

The study of the iron oxide activity in the slag under the proposed conditions of the green process should be helpful.